

U-Pb zircon age of Ediacaran Umarizal Granite Suite and emplacement mechanism with high-T hornfels generation in Jucurutu Formation, Borborema Province, NE, Brazil

Samir do Nascimento Valcácio^{1*} , Zorano Sérgio de Souza^{1,2} , Elson Paiva de Oliveira³ 

Abstract

The Borborema Province, NE Brazil, is marked by several Ediacaran granitic plutons that generated high-temperature metamorphic aureoles in the country rock. However, information about magma emplacement, age of plutonism, and metamorphic conditions are necessary to understand this scenario. To this end, we present field, petrographic, and zircon U-Pb geochronological data for migmatized hornfels and intrusive Umarizal and Tourão-Caraúbas plutons. The field features allowed the construction of a structural evolution model starting with high-temperature sinistral strike-slip shear zones followed by dextral strike-slip movement associated with the magmatic emplacement. Mineral paragenesis of andalusite/sillimanite, garnet, scapolite, and phlogopite in country rocks within the metamorphic aureole indicate temperatures of at least 700-800°C and pressures lower than 4.5 kbar corresponding to the pyroxene hornfels facies. Zircon U-Pb ages of 563.7 ± 6.2 for the Umarizal granite, 589 ± 4.4 Ma for the Tourão-Caraúbas granite, and 580.5 ± 4 Ma for the neosome from contact aureole were obtained. The results show that magma emplacement and HT/LP (high-T/low-P) contact metamorphism were synchronous with a transtensional event. These features suggest a late- to post-tectonic context, following the collapse of the Brasiliano/Pan-African orogenic chain, that favored Late Ediacaran plutonism and synchronous HT/LP metamorphism.

KEYWORDS: contact metamorphism; emplacement mechanism; U-Pb geochronology; Ediacaran plutonism.

INTRODUCTION

The Borborema Province (BP) resulted from the collision of two blocks, the Amazonian / São Francisco and the West Africa / São Luís cratons, with tectonic stabilization during the Brasiliano / Pan-African orogenesis (Almeida *et al.* 1981). This province is limited to the west by the Parnaíba Basin, to the north and east by Meso-Cenozoic sedimentary covers, and to the south by the São Francisco Craton (Fig. 1). This province is made up of a complex mosaic of variably migmatized tectonic blocks amalgamated during the Brasiliano / Pan-African collage. It shows an interconnected network of shear zones, which delimit a voluminous Neoproterozoic

intrusive magmatism (Vauchez *et al.* 1995, Brito Neves *et al.* 2000, Oliveira and Medeiros 2018).

Neoproterozoic magmatism has been subdivided according to structural, petrographic, geochemical, and geochronological data. In particular, for the Rio Grande do Norte Domain (RND), Nascimento *et al.* (2000, 2008, 2015) and Angelim *et al.* (2006) rearranged the various Ediacaran plutons into the following suites: Calc-Alkaline, Shoshonitic represented by São João do Sabugi pluton, High-K Calc-Alkaline Porphyritic represented by Itaporanga pluton, High-K Calc-Alkaline Equigranular represented by Dona Inês pluton, Alkaline represented by Catingueira pluton, and Alkaline Charnockitic represented by Umarizal pluton, the latter being the subject of this study (Fig. 2).

One striking feature of this Ediacaran plutonism is its time correlation with high-temperature (650-850°C) and low to medium pressure (3-5 kbar) contact metamorphism associated with anatexis and thermal aureoles over the adjacent host units (Galindo *et al.* 1995, Souza *et al.* 2006, 2017a, 2017b, Archanjo *et al.* 2013, Campos *et al.* 2016, Valcácio *et al.* 2017, Cunha *et al.* 2018). Mineral paragenesis such as sillimanite-andalusite-cordierite-scapolite-phlogopite-wollastonite-garnet are reported on the metamorphic contact (Lima *et al.* 1989, Sial 1989, Souza *et al.* 2007, Caby *et al.* 2009, Archanjo *et al.* 2013, Chagas *et al.* 2018).

This paper aims to provide new field, structural, petrographic, and zircon U-Pb geochronology data, in addition to a detailed description of the metamorphic paragenesis bordering the

¹Programa de Pós-Graduação em Geodinâmica e Geofísica, Universidade Federal do Rio Grande do Norte – Natal (RN), Brazil. E-mail: samir.valcacio@gmail.com

²Departamento de Geologia, Universidade Federal do Rio Grande do Norte – Natal (RN), Brazil. E-mail: zorano@geologia.ufrn.br

³Departamento de Geologia e Recursos Naturais, Instituto de Geociências, Universidade Estadual de Campinas – Campinas (SP), Brazil. E-mail: elsonapo@unicamp.br

*Corresponding author.

Supplementary data

Supplementary data associated with this article can be found in the online version: [Supplementary Table](#).



contact of the Umarizal pluton. Integration of these data with those available in the literature allows a better understanding of the structural and kinematics control as well as the pressure and temperature conditions involved in the emplacement of magmas at the end of the Neoproterozoic in this part of the RND. In this regard, the emplacement mechanism and the precise time interval of the high-temperature and low-pressure event observed on supracrustal host rocks are refined.

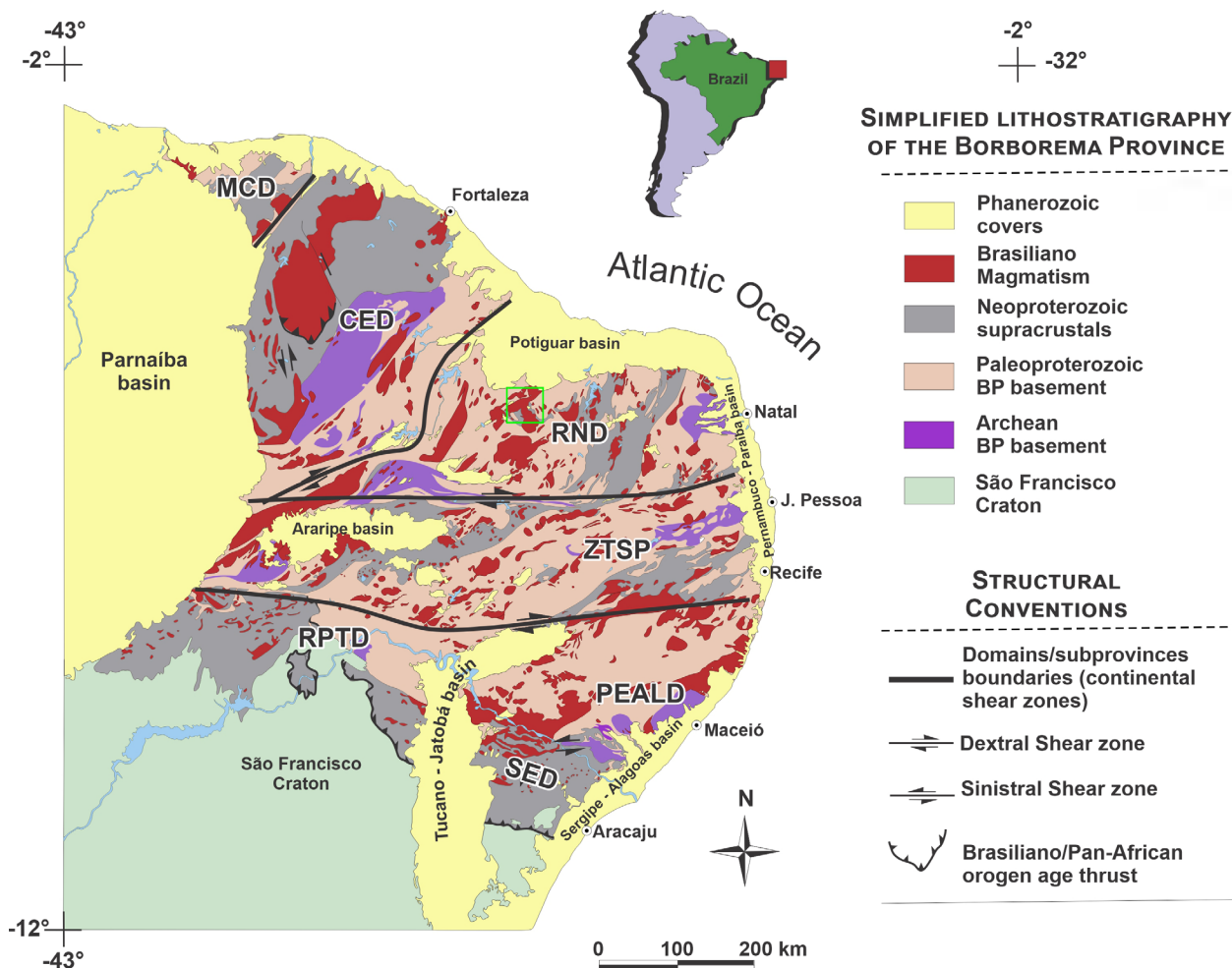
METHODS AND ANALYTICAL TECHNIQUES

This work was carried out through three distinct steps:

- careful review of available bibliographic and cartographic surveys including a compilation of available data from the regional literature and processing of digital images from aerial photographs (1:70,000 scale), and satellite images Landsat-7 / ETM+ and Landsat-8 / OLI;
- visit to key outcrops for a detailed description of lithological contacts, crosscutting relationships, and distribution of mineral phases related to the contact aureole;

- zircon U-Pb geochronology applied to both plutonic rocks and neosome of migmatized hornfels nearby intrusive contacts.

To conduct the last step, the samples were fragmented with a jaw crusher, followed by 250 mm grinding of these rocks, manual batting techniques, and mineral separation by methylene iodide and Frantz magnetic separator. Zircon grains were selected manually with a binocular loupe, mounted on epoxy resin, and, finally, imaged by cathodoluminescence. All of these procedures were conducted at the Geoscience Institute of Universidade de Campinas (IG / Unicamp). The isotopic data were also obtained at IG / Unicamp on an ICP-MS Element XR (Thermo Scientific) coupled to an Excite193 laser ablation system (Photon Machines) with HelEx ablation cell (25 μm laser beam). Data were reduced with the Iolite software and compared with the reference zircon 91500 (1065.4 ± 0.3 Ma; Wiedenbeck *et al.* 1995) and with the Peixe zircon (564 ± 4 Ma, Navarro *et al.* 2017) for data quality control.



MCD: Médio Coreaú Domain; CED: Ceará Domain; RND: Rio Grande do Norte Domain; PEALD: Pernambuco-Alagoas Domain; RPTB: Riacho do Pontal Belt; SEB: Sergipano Belt; CCD: Ceará Central Domain; AC: Acaraú; OJ: Orós-Jaguaribe; GSE: Granjeiro-Seridó; SE: Seridó; RP: Rio Piranhas; SJC: São José de Campestre; PAB: Piancó-Alto Brígida; AP: Alto Pajeú; AM: Alto Moxotó; RC: Rio Capibaribe; SP: São Pedro.

Figure 1. Geological map and simplified tectonic context of the Borborema Province (BP) with emphasis on the voluminous Brasiliano / Pan-African orogen age and thrust (compiled after Oliveira and Medeiros 2018). The schematic map in the lower right corner shows the BP compartmentation according to Santos and Medeiros (1999) and Santos *et al.* (2000).

GEOLOGICAL CONTEXT

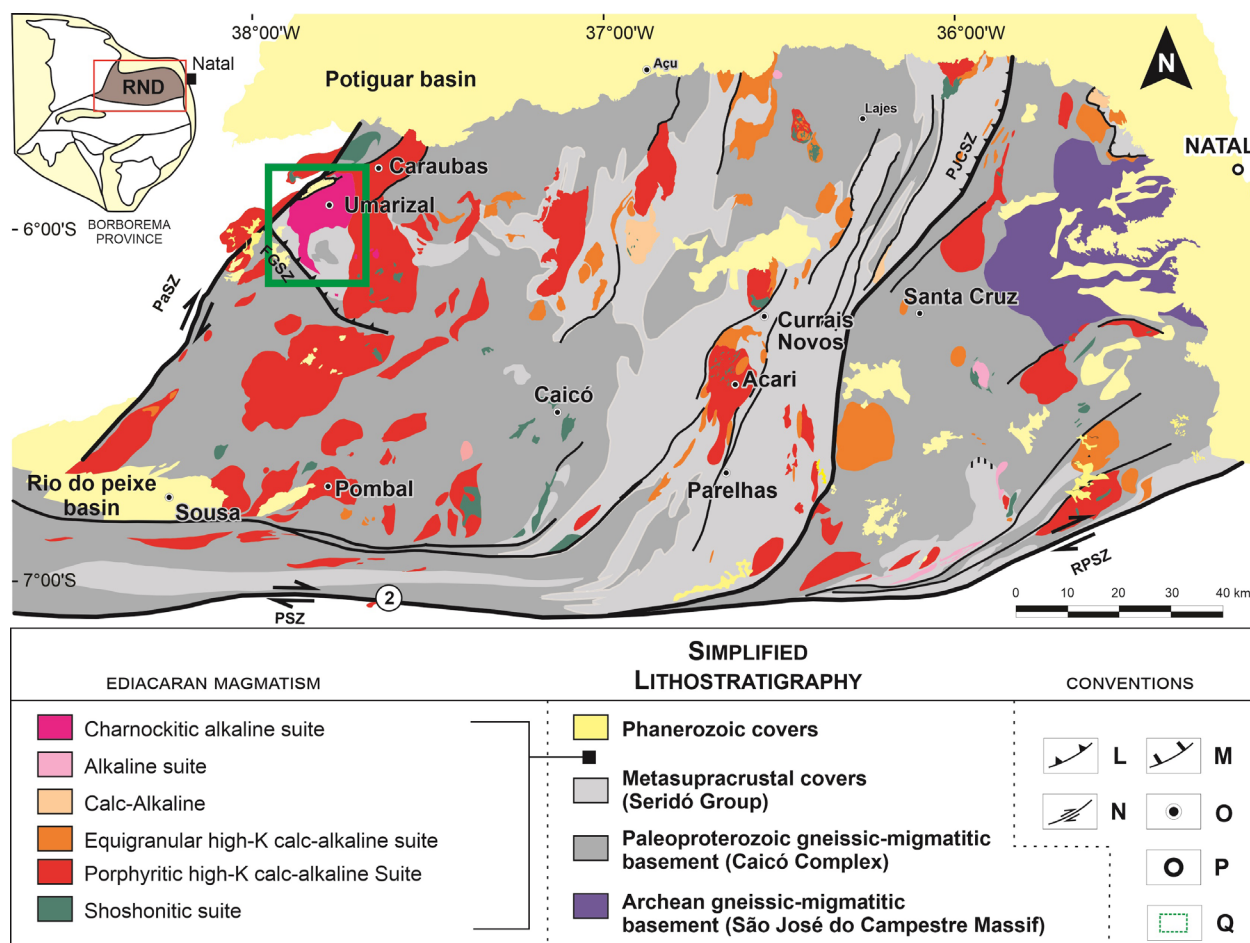
The study region is inserted in the Rio Grande do Norte Domain (RGND), northeastern of BP (Fig. 2). It consists of a Paleoproterozoic gneissic basement (Caicó Complex; Jardim de Sá 1984, 1994, Souza *et al.* 2007), over which Neoproterozoic metasedimentary sequences of the Seridó Group were deposited. This group is composed of three formations: Jucurutu (paragneisses with lenses of marble and calc-silicate rocks) at the base; Equador (quartzite and metaconglomerates) in the middle portion; and Seridó (micaschists) on top. These lithologies are intruded by plutonic bodies with distinct petrographic and geochemical characteristics (Silva *et al.* 2015, Valcácio *et al.* 2017). In the study area, the contact of the Umarizal pluton with the Jucurutu Formation host rocks is intrusive and marked by an expressive thermal aureole at the hornblende to pyroxene hornfels facies.

In this region, Portalegre (PaSZ) and Frutuoso Gomes (FGSZ) shear zones are interpreted as synchronous or late tectonic to the collision of São Francisco and Congo cratons, and probably controlled the emplacement of Ediacaran granitic plutons (Galindo *et al.* 1995, Vauchez *et al.* 1995, Archanjo *et al.* 1998, Trindade *et al.* 1999). According to Hackspacher and Legrand (1989), mineral associations and metamorphic textures indicate that mylonitization in the PaSZ reached

temperatures between 500-350°C and pressures of 5-2 kbar at greenschist facies; with an estimated geothermal gradient of ~20°C/km. However, porphyritic granite emplaced in the PaSZ displays mineral paragenesis compatible with the amphibolite facies, which suggests that the greenschist facies record would be linked to a later retrometamorphic event, unrelated to plutonism (McReath *et al.* 2002).

The geological mapping conducted in this research (Fig. 3) revealed that the Charnockitic Alkaline Suite (ChAlk) is composed of the main body, the Umarizal pluton, having an area of ~300 km², in addition to nearby smaller satellite occurrences. This pluton crosscuts the Caicó Complex, which is constituted by migmatitic gneisses, and metasedimentary rocks (biotite gneisses, marbles, calc-silicate gneisses) of the Jucurutu Formation and the Tourão-Caraúbas pluton (observed as stocks or dykes; Fig. 3). The best records of the contact metamorphism on country rocks adjacent to the pluton appear in paragneisses and marbles of the Jucurutu Formation (Fig. 4A). This metamorphic aureole is marked by andalusite and garnet porphyroblasts and acicular sillimanite (Figs. 4B and 4C), besides recrystallized granoblastic mosaics of calcite in marbles (Fig. 4D) with or without phlogopite.

Migmatized hornfels can develop banded (stromatic), schlieren, or nebulitic features. The contact between these



L: Neoproterozoic contractional-transpressional shear zones; M: Neoproterozoic extensional shear zones; N: Neoproterozoic transcurrent shear zones occurring; O: city; P: state capital; Q: study area; PaSZ: Portalegre shear zone; FGSZ: Frutuoso Gomes shear zone; PSZ: Patos shear zone; RPSZ: Remígio-Pocinhos shear zone; PJCSZ: Picuí - João Câmara shear zone.

Figure 2. Geological framework of the Rio Grande do Norte Domain emphasizing the Ediacaran plutonism (after Nascimento *et al.* 2000, 2008, 2015).

rocks and the Umarizal pluton is sharp or irregular, and on the edge of the pluton, there is decreasing grain size along the chilled margin, as it is common in intrusive bodies (Fig. 5A). In country rocks, neosomes vary in compositions from tonalite, biotite-garnet-bearing quartz syenite to granite. In these rocks, fine-grained (< 1 mm; Winter 2013), equigranular, granoblastic, and/or lepidoblastic texture and banded appearance are identified. In tonalitic type (Fig. 5B), its composition includes plagioclase, quartz, hornblende, and biotite. Quartz syenite neosome (Fig. 5C) is composed of quartz, plagioclase, K-feldspar, garnet, biotite, muscovite, titanite, and opaque. Granitic type (Fig. 5D) tends to be slightly porphyritic, and has K-feldspar, quartz, plagioclase, biotite, and minor garnet and opaque.

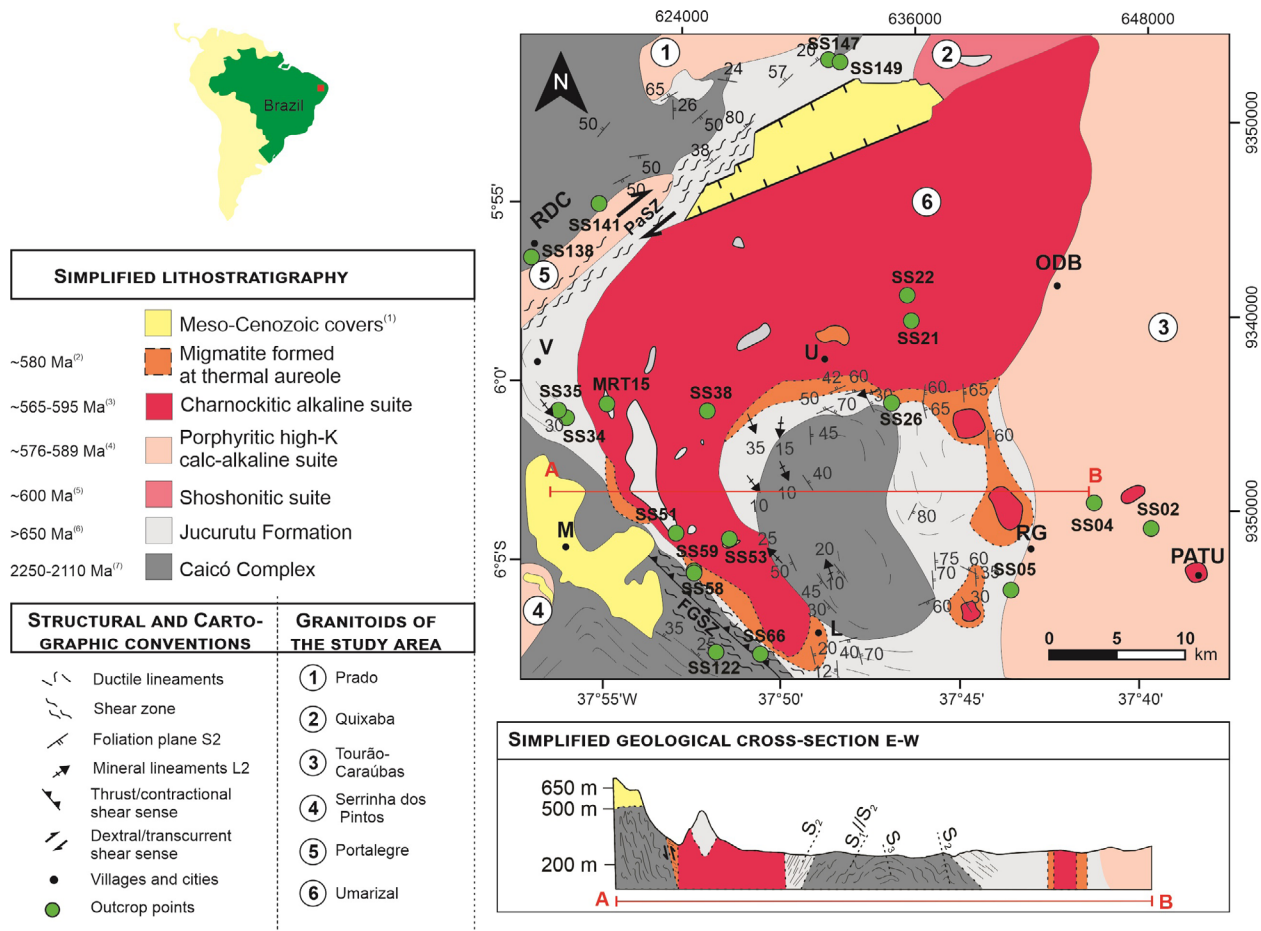
McReath *et al.* (2002) and Sá *et al.* (2014) published U-Pb zircon ages for the Umarizal pluton of, respectively, 593 ± 5 Ma and 601 ± 11 Ma. Souza *et al.* (2017b) reported zircon U-Pb Concordia age for a neosome close to the pluton border of 583 ± 1.8 Ma. The occurrence of microgranitic dykes of the Umarizal granite crosscutting the westward contact of the Tourão-Caraúbas batholith (Fig. 6), for which an earlier titanite U-Pb age of 580 ± 4 Ma is reported by Trindade *et al.* (1999), suggests that the different Ediacaran plutonism in the study region is coeval within a short time span of 10-5 m.a.

PETROGRAPHY

Umarizal granite

The Umarizal pluton encompasses three petrographic facies named Umarizal, Lagoa, and Açõ. The Umarizal facies corresponds to quartz monzonites and quartz syenite with fayalite and/or orthopyroxene and minor hedenbergite, Fe-edenite, and biotite. The accessory phases are allanite, magnetite, ilmenite, zircon, and apatite. The Açõ facies is restricted to the northeastern portion of the main body, and consists of monzogranites with quartz + hornblende symplectites, Fe-edenite and biotite, and accessory allanite, apatite, zircon, ilmenite, and titanite. Rapakivi varieties may occur occasionally (Galindo 1993, Galindo *et al.* 1995). The Lagoa Facies crops out as satellite bodies intrusive into the Tourão granite and has granite composition and mineralogy like those of the Açõ Facies. It shows fayalite-rich olivine with skeletal habit and partial resorption texture, besides forming double corona with grunerite and hornblende (Fig. 7A). Hornblende and vermicular quartz symplectites delineating a corona around diopside-hedenbergite (Fig. 7B), as well as myrmekite, perthite, and mesoperthite textures are also found.

Gabbro-norite is associated with the Umarizal pluton and form decimetric enclaves and small stocks with up to 0.2-0.5 km² of outcropping area. They have mafic mineralogy



PaSZ: Portalegre Shear Zone; FGSZ: Frutuoso Gomes shear zone; U: Umarizal; RG: Rafael Godeiro; P: Patu; MT: Martins; RDC: Riacho da Cruz; ODB: Olho d'Água Borges; L: Lucrécia.

Figure 3. Geological map of the study area with the location of outcrops mentioned in the text. References for geochronology data: (1) Angelim *et al.* (2006); (2) Souza *et al.* (2017b); (3) Galindo *et al.* (1995), McReath *et al.* (2002); (4) Trindade *et al.* (1999); (5) Sá *et al.* (2014); (6) Van Schmus *et al.* (2003); (7) Souza *et al.* (2016).

composed of orthopyroxene, clinopyroxene, and biotite, with diopside-hedenbergite and titanite as accessory phases. Hornblende and vermicular quartz symplectites also occur as corona in enstatite-rich pyroxenes, like those found in the Umarizal Granite.

Country rocks

Paragneisses, marbles, and calc-silicate gneisses from the Jucurutu Formation appear in the SW portion of the area or as mega xenoliths within the Umarizal pluton. Marbles and calc-silicates crop out as discontinuous NE-SW oriented lenses of kilometer-sized and extend to E-W when approaching the Patos Shear Zone. Microscopically, they show granoblastic, fine- to medium-grained equigranular texture, and vary from calcitic, pure marbles to impure types (Figs. 8A and 8B). There are continuous millimeter- to centimeter-thick bands defined by alternations of carbonate-rich (predominantly calcite) and actinolite- tremolite-rich layers, in addition to minor diopside-hedenbergite, phlogopite, and meionite-rich scapolite (Figs. 8C and 8D). Plagioclase, quartz, microcline, titanite, and epidote occur as accessories phases. Morais Neto (1987) and Archanjo *et al.* (1998) report occasional occurrences of forsterite-rich olivine and wollastonite.

Paragneisses occur in the S-SE portion and as mega xenoliths within the Umarizal pluton, both commonly partially

migmatized. They show migmatitic features extending up to 1-2 km from the contact with the intrusion. The mineralogical composition of paragneiss is marked by quartz, plagioclase, biotite, garnet, and sillimanite (Figs. 8E and 8F), besides andalusite, chlorite, muscovite, epidote, titanite, and hornblende as accessories.

ZIRCON U-Pb GEOCHRONOLOGY

Dating the Umarizal and Tourão-Caraúbas granites

Samples SS21 (Lat. 5°58'13"S / Long. 37°46'21"W) and SS4 (Lat. 6°3'30"S / Long. 37°41'42"W), from the Umarizal and Tourão-Caraúbas granite, respectively, were selected for zircon U-Pb dating (see Fig. 3). Sample SS21 is an isotropic coarse-grained quartz monzonite (Figs. 6A and 6B). Sample SS4 is a coarse-grained, inequigranular, porphyritic granite, in which microcline phenocrysts define an incipient magmatic lineation fabric (Fig. 6B).

U-Pb results for 54 spot analyses from the SS4 sample (Tourão-Caraúbas Granite) are shown in the Supplementary Table A1. Zircon grains show oscillatory or complex zoning, elongated prismatic habits and bipyramidal grain shape (Fig. 9A), with an average length (L) of $260 \pm 51 \mu\text{m}$, width (W)



Ns: Neosome; Grt: Garnet; Sil: Sillimanite; Fd: Feldspar; Qz: Quartz; Cal: Calcite.

Figure 4. Field features of the metamorphic aureole around the Umarizal pluton. (A) Intercalation of calcsilicate rocks and marbles from the Jucurutu Formation in xenolithic blocks with neosomes paralleling or truncating the S_2 foliation (point SSS1, SW of the study area). (B) and (C) Centimetric garnet porphyroblasts and sillimanite aggregates (point SS34, west of the study area). (D) Centimetric calcite megacrystals forming granoblastic mosaics at ~ 700 m from the contact (point SS35, west of the study area); the metallic tip of the hammer points to the north.

of $96 \pm 20 \mu\text{m}$, and L/W ratios = 2.8 ± 0.6 , and $\text{Th}/\text{U} = 0.86 \pm 0.48$ ($\text{Th} = 297 \pm 158 \text{ ppm}$, $\text{U} = 446 \pm 37 \text{ ppm}$). A group of 35 grains with $< 5\%$ of discordance resulted in a weighted average $^{206}\text{Pb}/^{238}\text{U}$ age of $589.3 \pm 4.4 \text{ Ma}$ ($\text{MSWD} = 3.7$; Fig. 9B). This date is interpreted as the age of the intrusion.

U-Pb results of 48 spot analyses from the SS21 sample (Umarizal granite) are shown in Supplementary Table A2. Zircon

grains have an average length (L) of $244 \pm 56 \mu\text{m}$, width (W) of $76 \pm 18 \mu\text{m}$, and L/W ratios = 3.3 ± 1.0 and Th / U of 0.58 ± 0.11 ($\text{Th} = 99 \pm 199 \text{ ppm}$, $\text{U} = 194 \pm 474 \text{ ppm}$). They are generally euhedral, elongated prismatic crystals, homogeneous, usually zoned due to overgrowth slightly younger rims, suggestive of continuous crystallization of two generations of zircon, with some grains exhibiting older internal portions (Fig. 10A). This

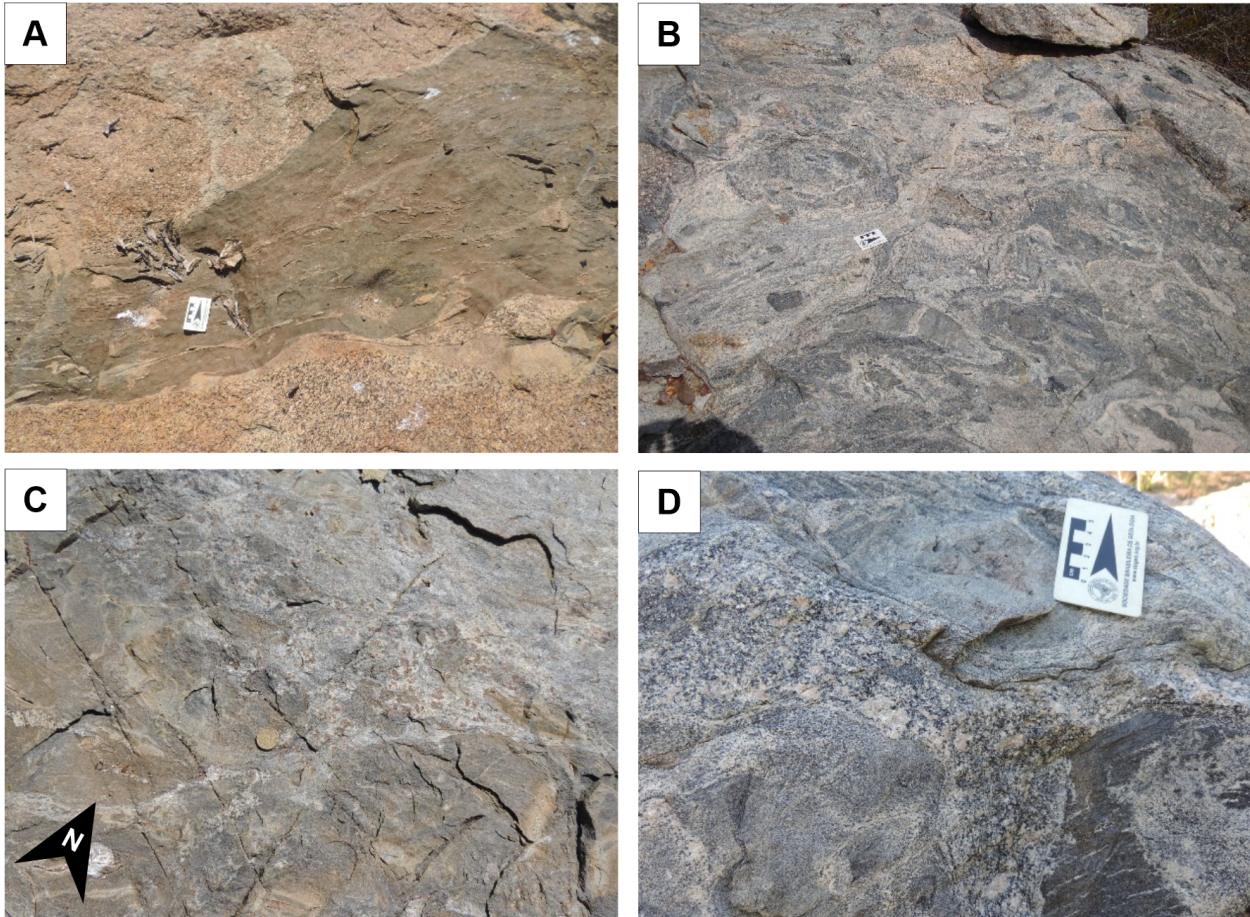


Figure 5. Metamorphic textures of the thermal aureole. (A) Relationship of Umarizal granite with paragneiss of the Jucurutu Formation; there is a thin cooling rim at the contact (point SSS, SE of the study area). (B) Migmatization of paragneiss forming leucogranite neosome (point SS58, SW border of the Umarizal pluton). (C) Migmatization of paragneiss forming peraluminous garnet-rich neosome (point SS53, SW of the study area). (D) Migmatite affecting paragneiss and generating slightly porphyritic neosome (point SS59, SW border of Umarizal pluton).

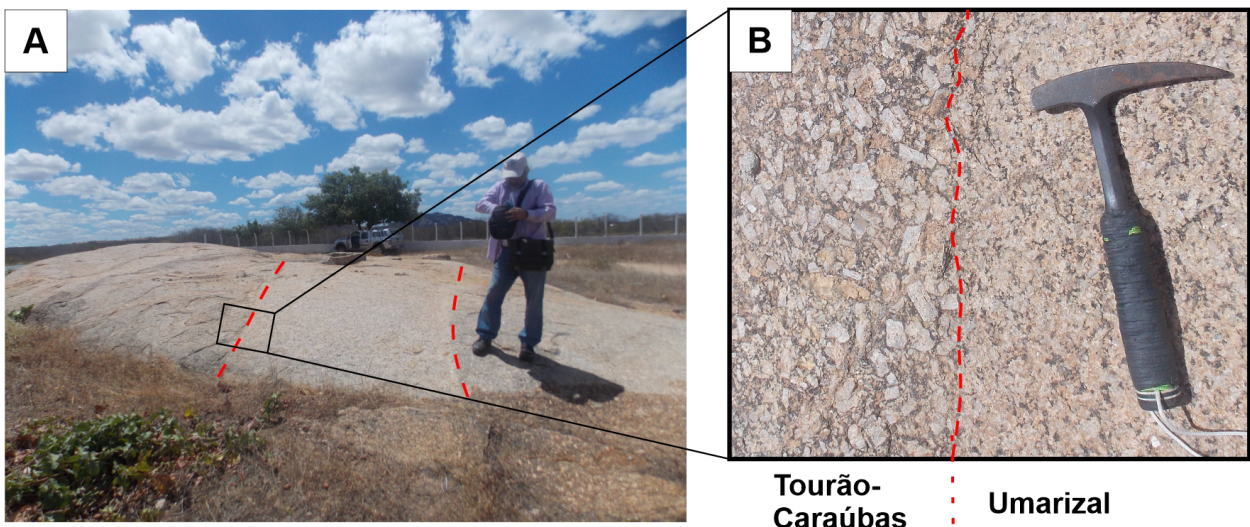


Figure 6. Contact relationship between the Umarizal and Tourão-Caraúbas granites. (A) Equigranular granite dyke of the Umarizal type crosscutting the Tourão-Caraúbas porphyritic granite. (B) Detail of (A). The metallic tip of the hammer indicates the north (point SS02, north exit of Patu).

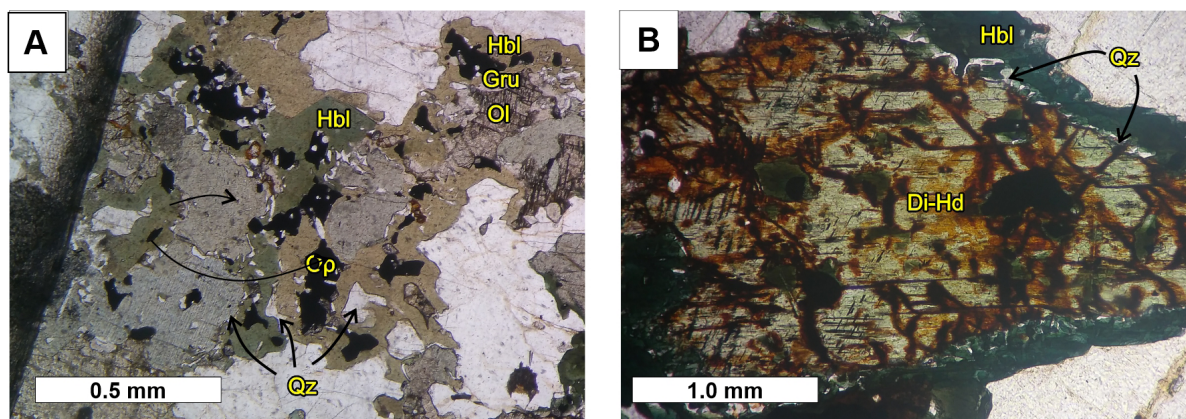
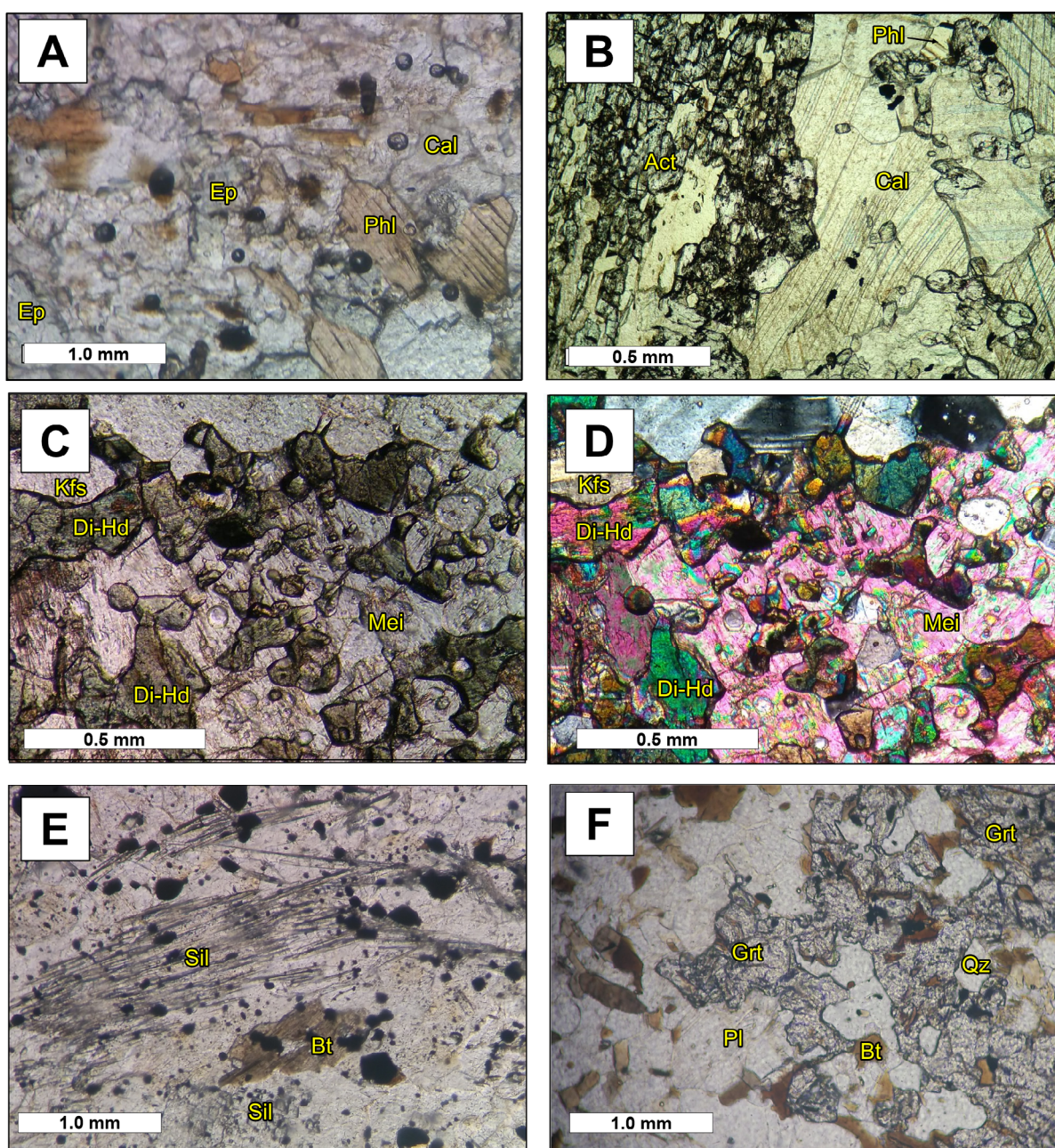


Figure 7. Microtextures of the central portion of the Umarizal pluton. (A) Double corona texture over olivine (Ol); the first fine and irregular layer is grunerite (Gru) and the second, thicker, is hornblende (Hbl). (B) Symplectite hornblende (Hbl) + quartz (Qtz) around diopside-hedenbergite (Di-Hd). Point SS21 in (A) and SS22 in (B). Both pictures were taken with uncrossed polarizers.



Di-Hd: diopside-hedenbergite; Mei: meionite; Sil: sillimanite; Bt: biotite; Grt: garnet; Pl: plagioclase; Ep: epidote; Qtz: quartz.
Figure 8. (A and B) Photomicrographs of marbles, (C and D) calcsilicate, and (E and F) biotite-bearing gneisses from the contact zone of the Umarizal pluton. (A) Epidote and phlogopite in impure marble. (B) Layers of granoblastic calcite and actinolite. (C) and (D) Meionite-rich scapolite poikiloblastic encompassing clinopyroxene. (E) Development of sillimanite from biotite. (F) Garnet poikiloblast in migmatitic neosome of paragneiss. Samples: SS34 (A, B), MRT15 (C) SS38 (D), SS26 (E, F). Uncrossed polarizers in (A), (B), (C), (E), and (F) and crossed polarizers in (D).

is reflected in the high error in calculated ages. Spots analyses < 10% discordant (Fig. 10B) provide a $^{206}\text{Pb}/^{238}\text{U}$ weighted average age of 565 ± 22 Ma (MSWD = 2.3). However, using a probability diagram for $^{206}\text{Pb}/^{238}\text{U}$ age distribution for the spots with < 5% disagreement (Fig. 11A), two distinct groups are observed, within the error range, and with very good statistical parameters. Four spots from a younger group, characterized by oscillatory zonation, corresponding to the grain edge (Fig. 11B), resulted in a $^{206}\text{Pb}/^{238}\text{U}$ weighted average of 563.7 ± 6.2 Ma (MSWD = 0.21). The oldest group, observed in homogeneous zircons or core portions, which may have patchy-type zoning (Fig. 11B), encompassing 32 spots, produced a $^{206}\text{Pb}/^{238}\text{U}$ weighted average of 587.2 ± 2.3 Ma (MSWD = 0.98). A third group, aged > 600 Ma, is considered here as an inheritance. The youngest age (563.7 ± 6.2 Ma) may represent the age of the Umarizal granite, the other dates are interpreted here as inherited ages. An alternative interpretation would be to interpret zircons with 587.2 ± 2.3 Ma as antecrystals (Davidson *et al.* 2007) possibly related to a mixture of the Umarizal and Tourão-Caraúbas felsic magmas.

Dating a neosome of migmatized hornfels at the border of Umarizal Granite

Sample SS59B was collected from the SW contact of the Umarizal pluton. It represents a neosome resulted from the partial melting of biotite-garnet-bearing paragneiss of the Jucurutu Formation. This neosome occurs as injections truncating the paragneiss paleosome and has occasional porphyritic texture marked by microcline phenocrysts (Fig. 5D). Data for 46 spots analyses are shown in the Supplementary Table A3. Zircon grains are prismatic (Fig. 12A), usually bipyramidal, elongated, with mean length (L) and width (W) of, respectively, 261 ± 67 μm and 67 ± 16 μm , and L/W ratio of 4.0 ± 11 . They show oscillatory zoning and form a homogeneous population with Th/U ratios of 1.36 ± 0.43 (Th = 215 ± 155 ppm, U = 157 ± 94 ppm), being interpreted as new zircon generated in the fusion process of thermal metamorphism. Spots with <5% discordance provided a Concordia age of 583.8 ± 1.8 Ma (MSWD = 4.0) and a $^{206}\text{Pb}/^{238}\text{U}$ pooled mean age of 580.5 ± 4.0 Ma (Fig. 12B). The latter is interpreted as the age of the thermal event.

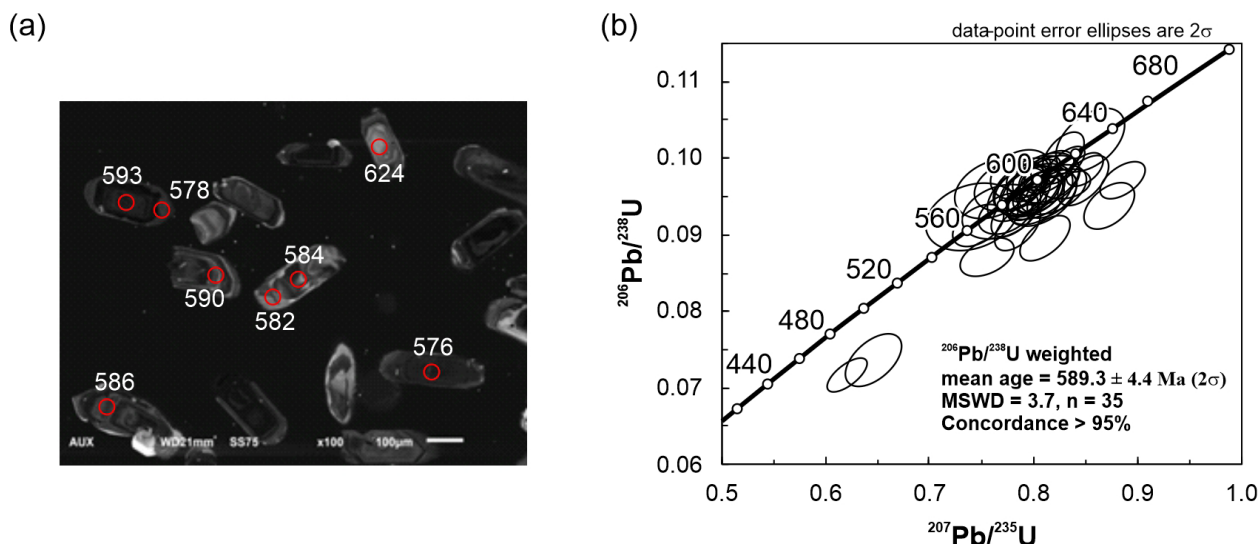


Figure 9. Zircon U-Pb result for the Tourão-Caraúbas granite (sample SS4). (A) Zircon cathodoluminescence images (spot age in Ma). (B) Concordia plot and weighted average age $^{206}\text{Pb}/^{238}\text{U}$ of concordant zircons (> 95% concordance).

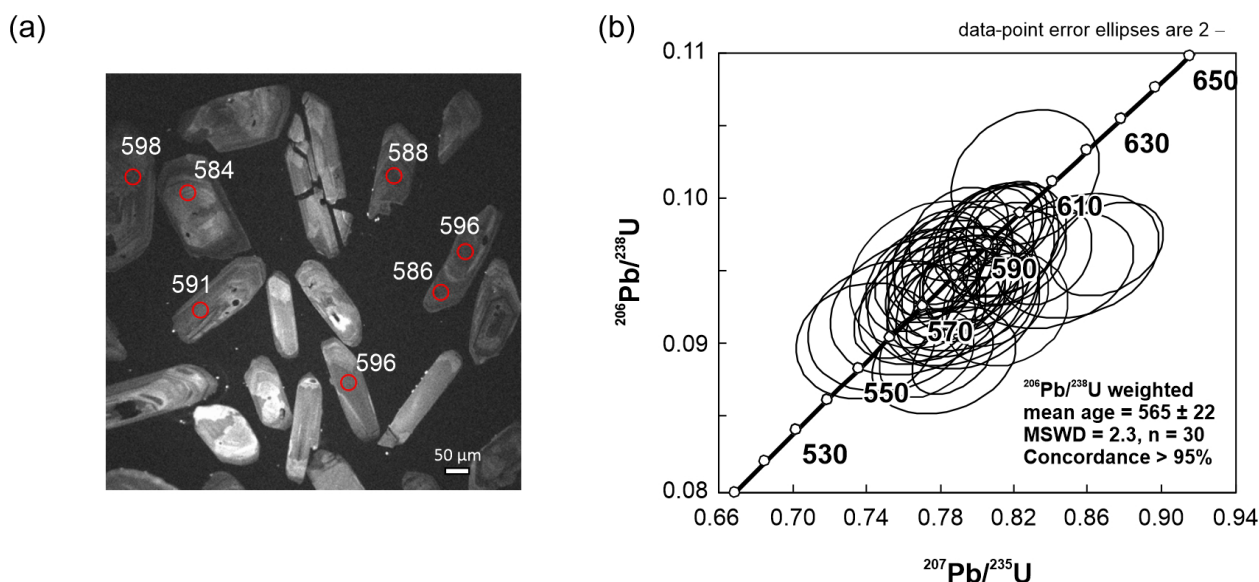


Figure 10. Zircon U-Pb dating of Umarizal granite (sample SS21). (A) Zircon cathodoluminescence images (spot age in Ma). (B) Concordia plot diagram and weighted average age $^{206}\text{Pb}/^{238}\text{U}$ of concordant zircons (> 95% concordance).

TECTONO-METAMORPHIC CHARACTERIZATION

The structural framework of the region is characterized by three tectono-metamorphic events. The oldest events, called D_1 and D_2 , are interpreted to have happened prior to the Umarizal and Tourão-Caraúbas plutonism. The younger event (D_3) includes an extensional stage that favored the opening of space for the emplacement of the magmas that originated the Umarizal and Tourão-Caraúbas granites and was taken as concomitant with the contact metamorphism of the country rocks (event Mc). The D_3 event ended with space closure and reactivation of ductile shear zones. Finally, a brittle deformation (D_4) is registered by faults, breccias, and cataclases, corresponding to the reactivation of ancient structures during the Phanerozoic.

The oldest event (D_1) is recorded only in basement gneisses (the Caicó Complex). It is characterized by a low-angle metamorphic banding (S_1) with metamorphic paragenesis (M_1) of the upper amphibolite facies (Yardley 1989, Winter 2013), including recrystallization of feldspars and hornblende and

different degrees of migmatization. This tectono-metamorphic event (D_1/M_1) is marked by the paragenesis:

- biotite + hastingsite + plagioclase + quartz, in augen gneisses;
- biotite + microcline + plagioclase + quartz, in orthogneisses.

The second event (D_2) affects D_1 structures, generating closed to tight, isoclinal, recumbent folds (Fig. 13A), with low-angle axial plane foliation (S_2), which is also recorded as the first tectono-metamorphic event in the supracrustals sequence of the Jucurutu Formation (Fig. 13B). The metamorphism M_2 associated with D_2 also reached the amphibolite facies (Yardley 1989, Winter 2013), as described by the proposed associations below:

- hornblende + plagioclase, in biotite gneisses;
- tremolite + actinolite + diopside + calcite + titanite + plagioclase + quartz, in calc-silicate rocks;
- tremolite + quartz + diopside, in marbles.

Stereographic projections of D_2 structures (S_2 foliation and L_2 lineation) and D_3 (S_3 foliation and L_3 lineation) of the

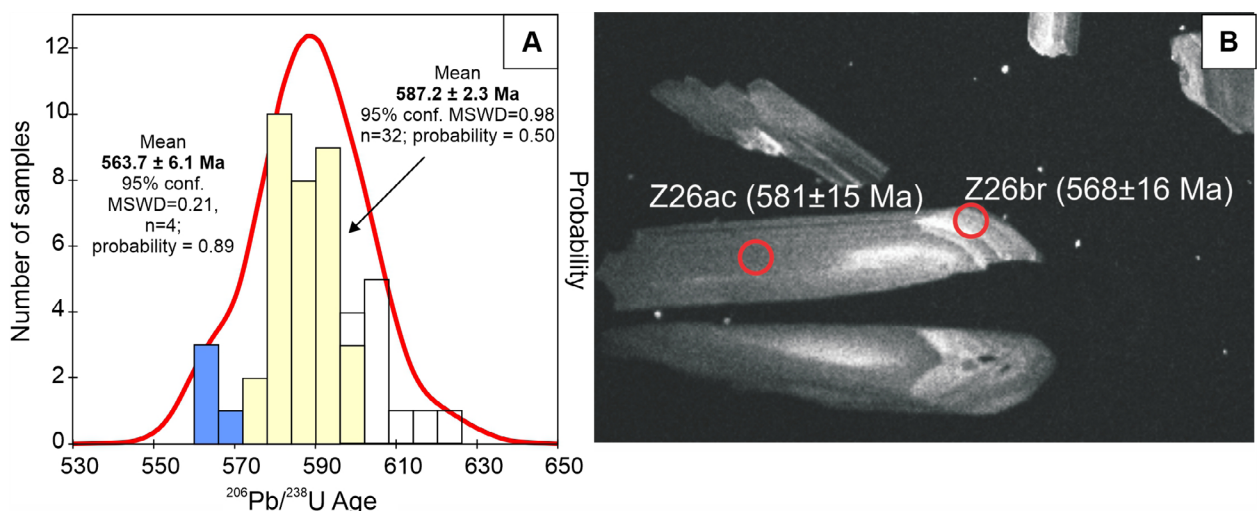


Figure 11. $^{206}\text{Pb}/^{238}\text{U}$ age distribution diagram of zircons from sample SS21 in (A); and grain cathodoluminescence image illustrating younger edge (spots S21_27 and S21_28 in Appendix A2) in (B).

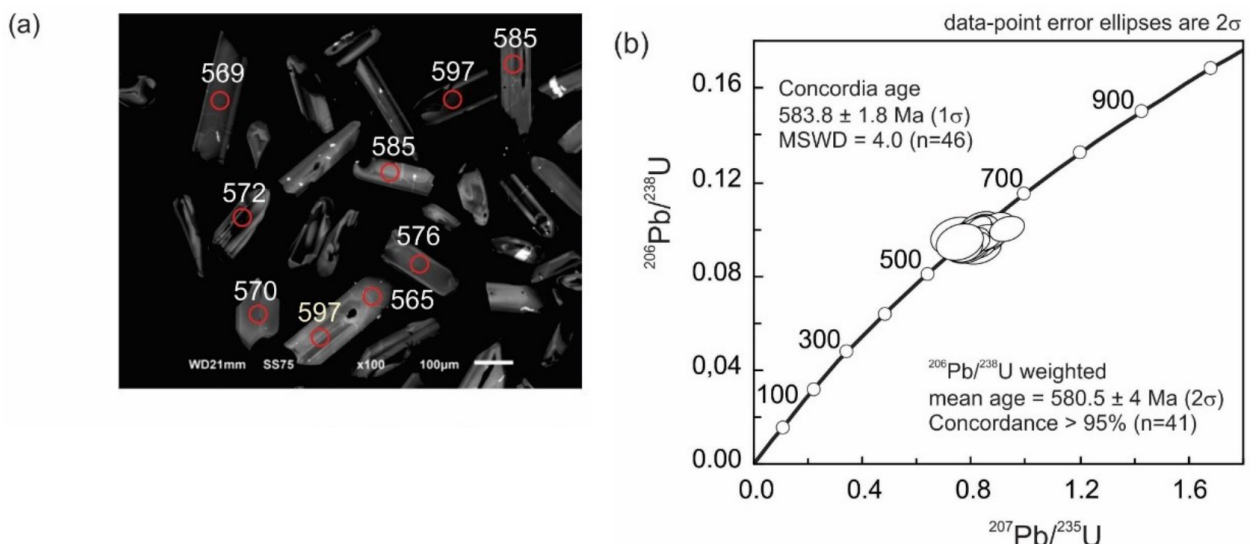


Figure 12. Zircon U-Pb dating result for neosome S59B. (A) Zircon cathodoluminescence images (spot age in Ma). (B) Concordia and weighted average $^{206}\text{Pb}/^{238}\text{U}$ ages of concordant zircons (> 95% concordance).

studied region were subdivided into three distinct sectors (Fig. 14), described as follows:

- the PaSZ to the north and northwest;
- the FGSZ to the west and southwest;
- the south of the pluton.

These structural sectors are shown in Figure 14 with the respective projections of structures D_2 and D_3 . The strike of S_2 for most structures agrees with the NE trend of the FGSZ region, with smooth dip, while the PaSZ region has two main structure groups, one with NE-SW direction and strong dip and another with SE strike and dip varying from weak to strong. The southern region of Umarizal also has two main groups, one with ENE-WSW direction and another with E-W direction, with dip changing from weak to strong.

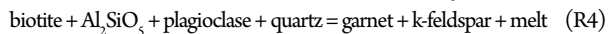
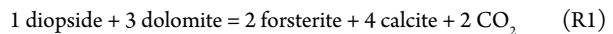
The S_3 structures in the FGSZ region dip mainly to NNW. No such structures were found in the PaSZ region. The third event (D_3) is interpreted as being progressive in two stages. The first stage, here called D_{3A} , is related to a regional distention system, with displacement components to ESE in the SW portion and to NNE in the NW part, which allowed the alkaline charnockite suite to be accommodated synchronously or in the late stage of D_{3A} . This event is accompanied by high-temperature metamorphism with an injection of nearly concordant neosomes within the gneissic banding and is here linked to the movement of the PaSZ and FGSZ, which delimit the Umarizal pluton. The PaSZ, north of the pluton, has a NE-SW direction and lengthens from the Rio do Peixe Basin (~ 120 km SW of Umarizal) to the Cretaceous Potiguar Basin (~ 25 km NW of Umarizal; Fig. 2).

The D_{3A} event is responsible for the formation of a subvertical foliation and a subhorizontal stretching lineation in the PaSZ. This area is marked by low-angle extensional shear bands with an indication of transport toward SE (Fig. 15A). The FGSZ, to the west, has an NW-SE direction, curving in the region of Martins to Frutuoso Gomes; it presents a smooth to moderate dip toward NE and predominance of sinistral S/C structures filled with granite neosome (Fig. 15B). The arrangement of these structures suggests that the block east of the FGSZ and south of the PaSZ moved eastward during the D_{3A} stage. This movement would have generated synformal and antiformal folds with

NW-SE directed axial plane S_3 and low angle S/C structures, which opened space for the accommodation of the Umarizal granite, triggering the contact metamorphism process (M_C). This metamorphic event resulted in recrystallization of previous phases and the appearance of the following hornblende to pyroxene hornfels facies paragenesis near pluton contact (< 2 km):

- meionite-rich scapolite + calcite + garnet in calc-silicate rocks;
- diopside + phlogopite + calcite in marbles;
- sillimanite/andalusite + garnet in biotite-gneisses and migmatites derived.

Following Morais Neto (1987) and Archanjo *et al.* (1998), forsterite and wollastonite in marbles and calc-silicates, and orthopyroxene in leucosomes of the Caicó Complex orthogneisses were also ascribed to the M_C event. Kase and Metz (1980) report the equilibrium of forsterite for a temperature range of 530-750°C (reaction R1 below). According to Spear (1995), the growth of orthopyroxene can be linked to the reaction R2 with stability curves between 700 and 800°C and pressure of 0.5 to 16 kbar. On the other hand, the presence of sillimanite / andalusite in partially migmatized biotite-gneisses or pluton mega xenoliths may be related, according to Spear (1995), with partial fusion reactions R3 and R4, under temperature conditions above the temperature of the hydrated granite solidus and pressures < 4 kbar.



The second stage, here called D_{3B} , is related to a contractional system that overlapped the previous one. It is evidenced by clockwise strike-slip reactivation of the PaSZ and thrusting in the FGSZ. Macrofolds developed in this stage are commonly symmetrical with normal and open style. Lineations related to D_{3B} show a smooth dip to NE (Fig. 14). This event is also marked by asymmetric porphyroclasts with pressure shadow, recrystallization tail, and S/C shear bands (Fig. 15C). The M_3 metamorphism, related to D_{3B} , has a retrometamorphic

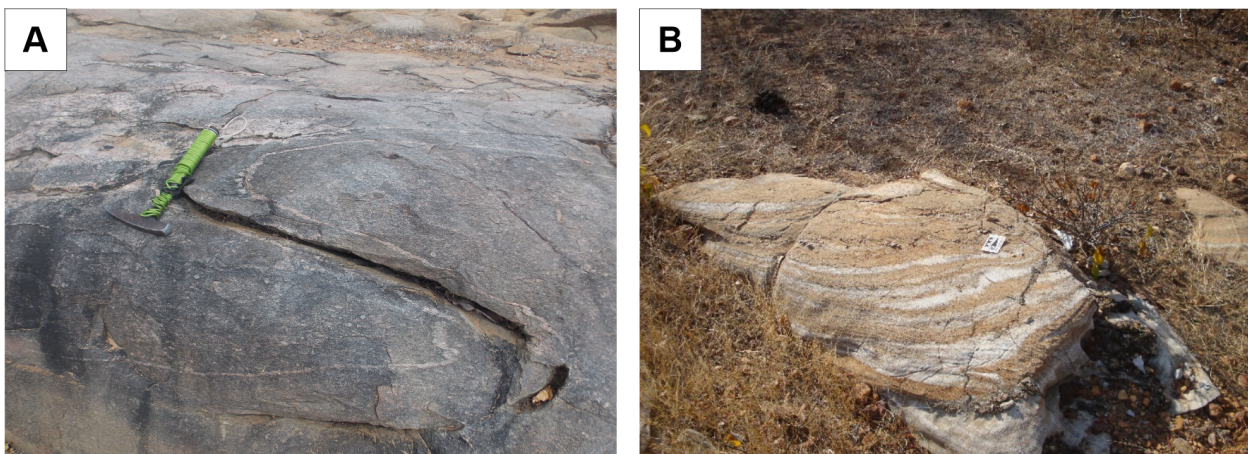


Figure 13. Structures recognized in the area. (A) Recumbent fold D2 in gneiss of the Paleoproterozoic Caicó Complex basement. (B) Metamorphic banding S_2 in marble of the Jucurutu Formation. Outcrops SS141 (A) and SS149 (B), NW portion of the area. The metallic tip of the hammer points to the north in (A).

character, in the greenschist facies (Yardley 1989, Winter 2013), evidenced by epidotization of plagioclase and chloritization of biotite and hornblende. This tectono-metamorphic event (D_{3B}/M_3) is associated with the following mineral associations:

- biotite + muscovite + chlorite in calc-silicate rocks;
- biotite + muscovite in biotite-gneisses and orthogneisses;
- epidote + titanite and opaque in biotite-gneisses, marbles and augen gneisses;

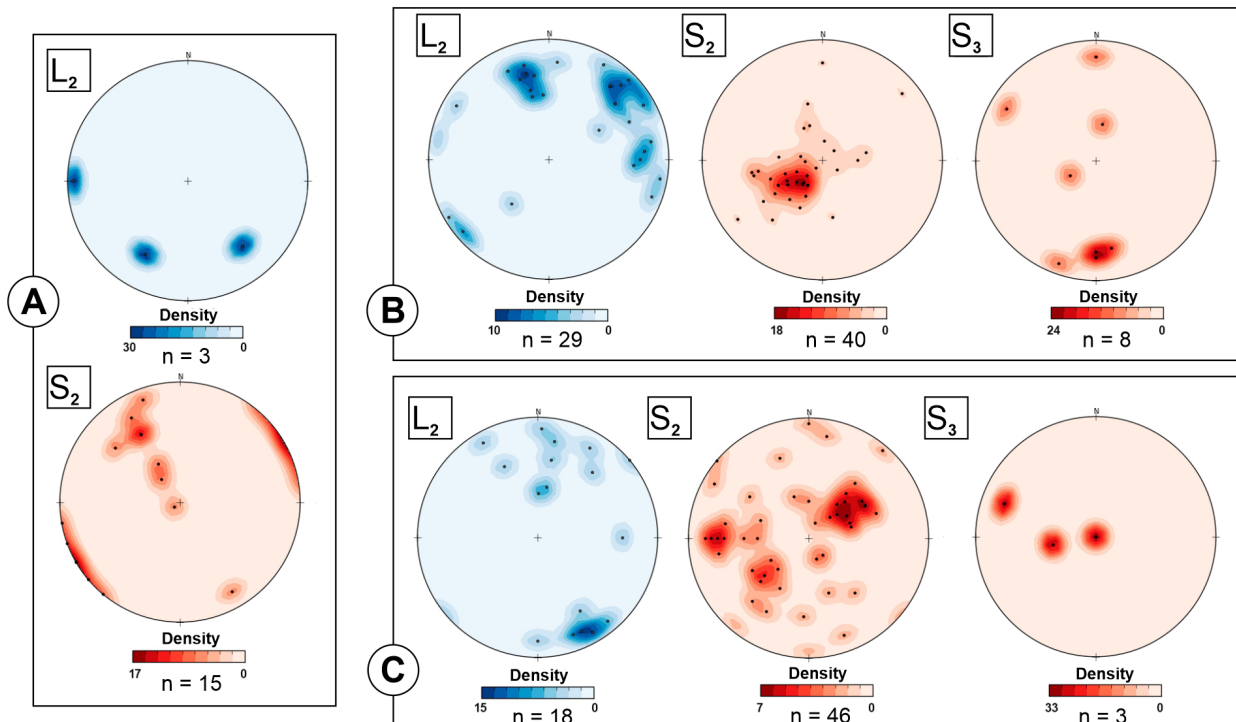
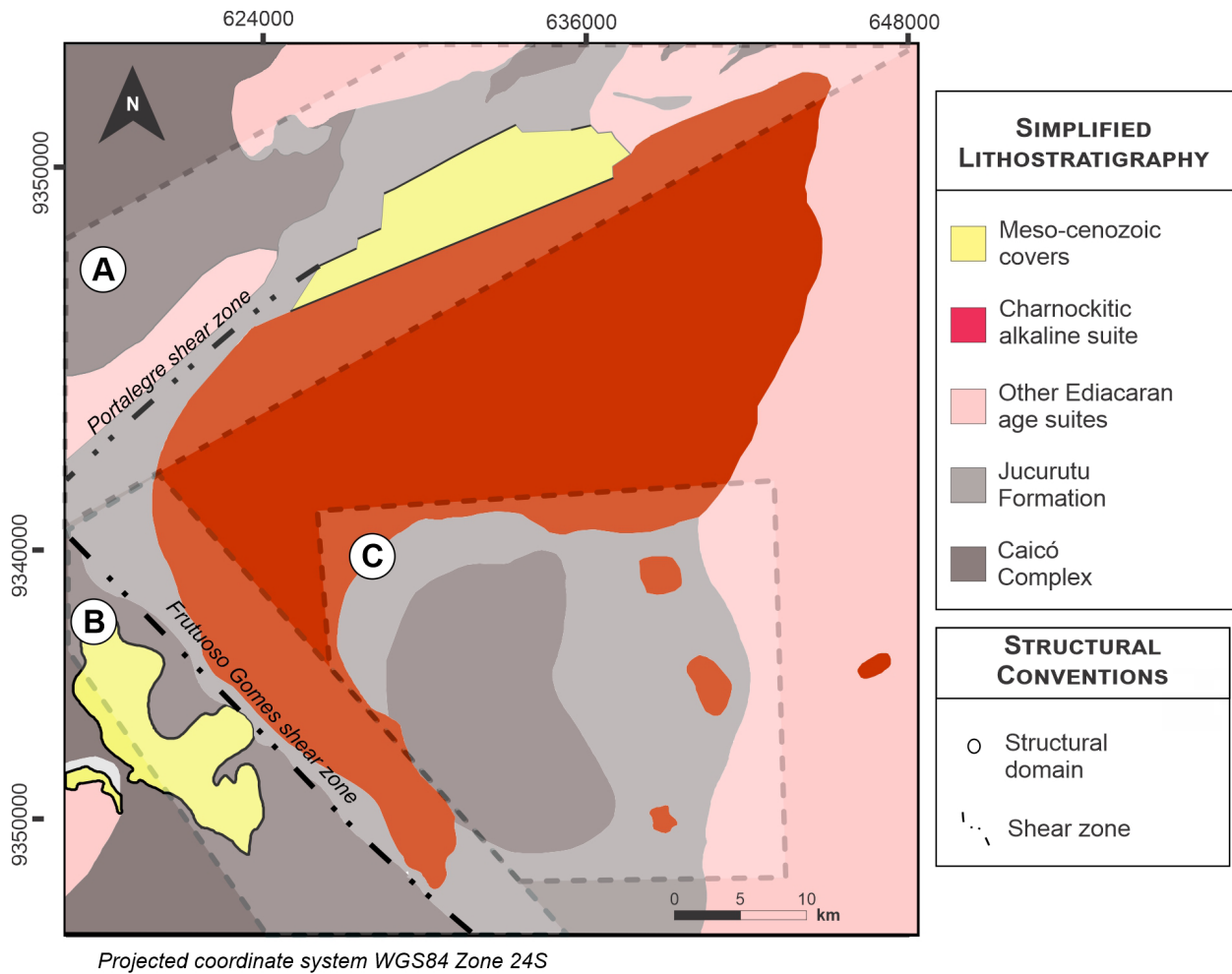


Figure 14. Location of the main structural domains recognized in the study area and stereographic projections corresponding to S_2 and S_3 foliations and L_2 lineation. Structural domains: (A) Portalegre shear zone; (B) Frutuoso Gomes shear zone; (C) southern Umarizal region.

Figure 16 outlines an integrated model of evolution considering the structures described above.

DISCUSSION

Metamorphic P-T conditions associated with the plutonism

Zircon U-Pb dating and petrographic data from migmatized hornfels, metapelites, and granites having contact aureoles in various places of the Borborema Province, in addition

to the synchronous (re)activation of a ductile shear zone in a context of high-temperature / low-pressure (HT / LP) conditions, are reported in the literature. These results point out to an important and expressive peak of regional high-grade metamorphic episodes during the Ediacaran (Souza *et al.* 2006, Archanjo *et al.* 2013).

In paragneisses, mineral associations of the hornblende to pyroxene hornfels occur, locally with garnet (almandine), scapolite, sillimanite / andalusite, and rare hypersthene. Several places show incipient to extensive migmatization of paragneisses, which imply that the partial melting curve for

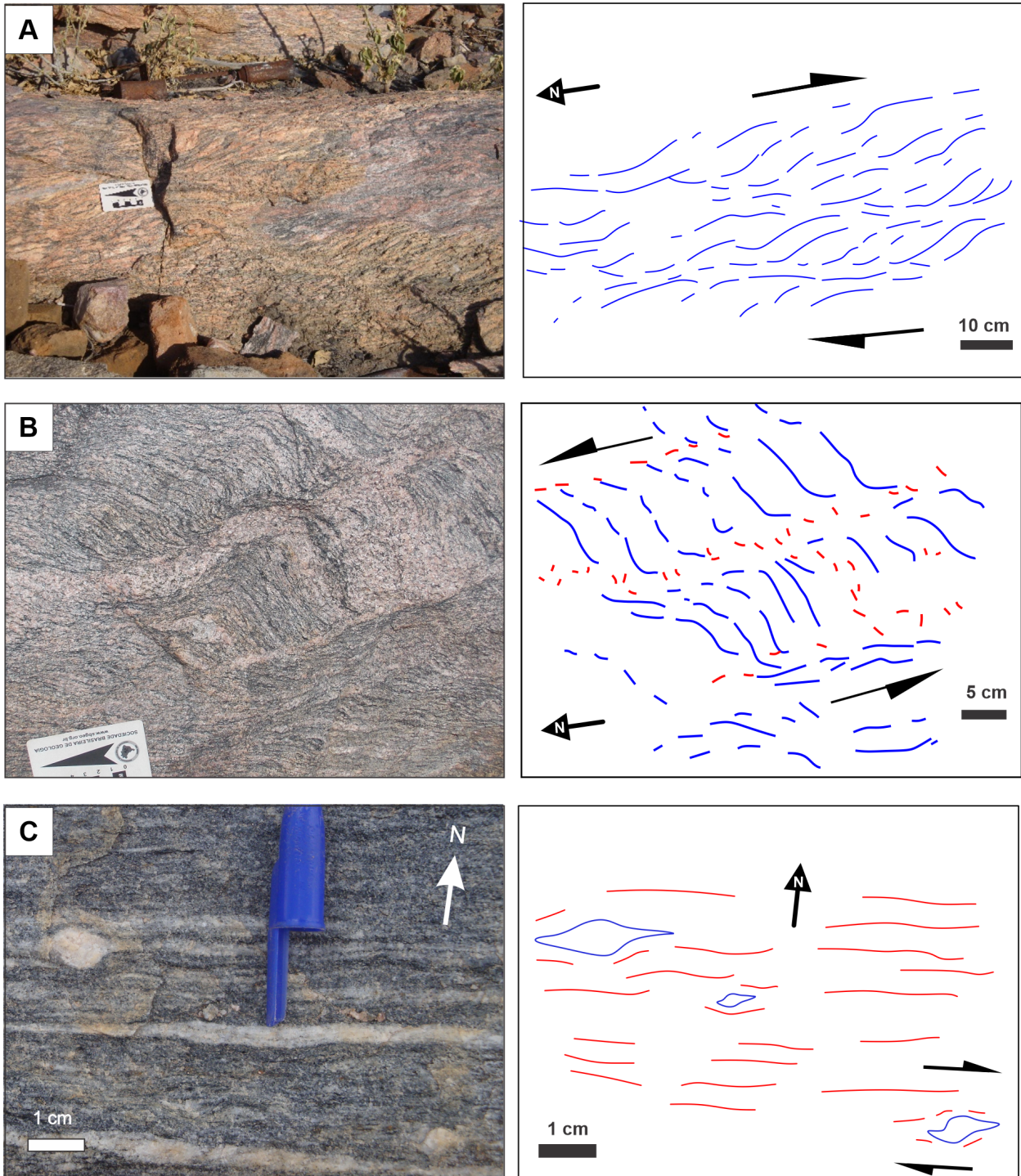


Figure 15. Kinematic indicators observed in shear zones. (A) Extensional clockwise S/C composite structure (seen in a vertical plane) in basement gneiss, indicating tectonic transport toward SSE (point SS147, north of study the area). (B) Shear bands with anti-clockwise kinematics (seen in vertical section), indicating extensional movement component with transport toward NE (point SS66, SW of the study area). (C) Clockwise movement (seen in a horizontal plane), recorded in K-feldspar phenocrysts (point SS138, NW of the study area).

hydrated granite system has been reached and, thus, indicate temperatures of at least 620-700°C and maximum pressures of 4.0 kbar (Yardley 1989, Winter 2013). In pure marbles, there is a progressive increase in grain size, whilst in impure marble and calc-silicate rocks, the formation of meionite-rich scapolite is prominent, implying temperatures above 800°C (Newton and Goldsmith 1976, Moecher and Essene 1990, Almeida and Jenkins 2017). Such mineral associations may reflect that the peak of temperature crossed the pyroxene hornfels facies and the anatexis isograd (Yardley 1989, Winter 2013). The occurrence of andalusite and the absence of kyanite and synchronous tectonic fabric, combined with the presence of hornfels along with the pluton intrusion, suggest pressures below 4.5 kbar (Holdaway 1971, Pattison 2001, Pattison *et al.* 2002, Winter 2013). This means a shallow depth for magma emplacement, at the middle to upper continental crust. The presence of fayalite only in the central portion of the Umarizal pluton could reflect slightly warmer conditions in this region (> 750°C) during magma cooling or some barrier keeping it from hydration (Bucher and Frost 2006, Frost and Frost 2008).

Temperature conditions for the formation of the textures and minerals described above are consistent with an HT / LP metamorphic environment associated with anhydrous intrusions (Winter 2013). The effect of the thermal metamorphism

occurs to about 1-2 km from the pluton contact. Additionally, the occurrence of both angular paleosome and rounded and/or deformed fragments from the host rocks along the pluton contact may imply complex processes of emplacement and could involve superposition of emplacement mechanisms (Barton *et al.* 1991, Brown and Solar, 1998, 1999).

The thermal event and its continental extension

Integration of our new U-Pb zircon geochronological data with previously published results suggest interpreting the geological context of the studied region as follows:

- chronocorrelation of Ediacaran magmatic pulses of the Umarizal region in the time range of 580-560 Ma;
- the Umarizal suite has an age of 564 Ma, with its other zircons aged 580-600 Ma, inherited from the Tourão-Caraúbas, and the 587 Ma zircons being antecrystals from this pluton.

Table 1 summarizes the modal, geochemical, and mineral chemistry between the Tourão-Caraúbas and Umarizal granitoids, based on Galindo (1993), Campos *et al.* (2016), and our data reported here. The Umarizal magmatism shows rare-earth patterns very similar to those of the Tourão-Caraúbas granitoid, although they are distinct in geochemical and petrographic

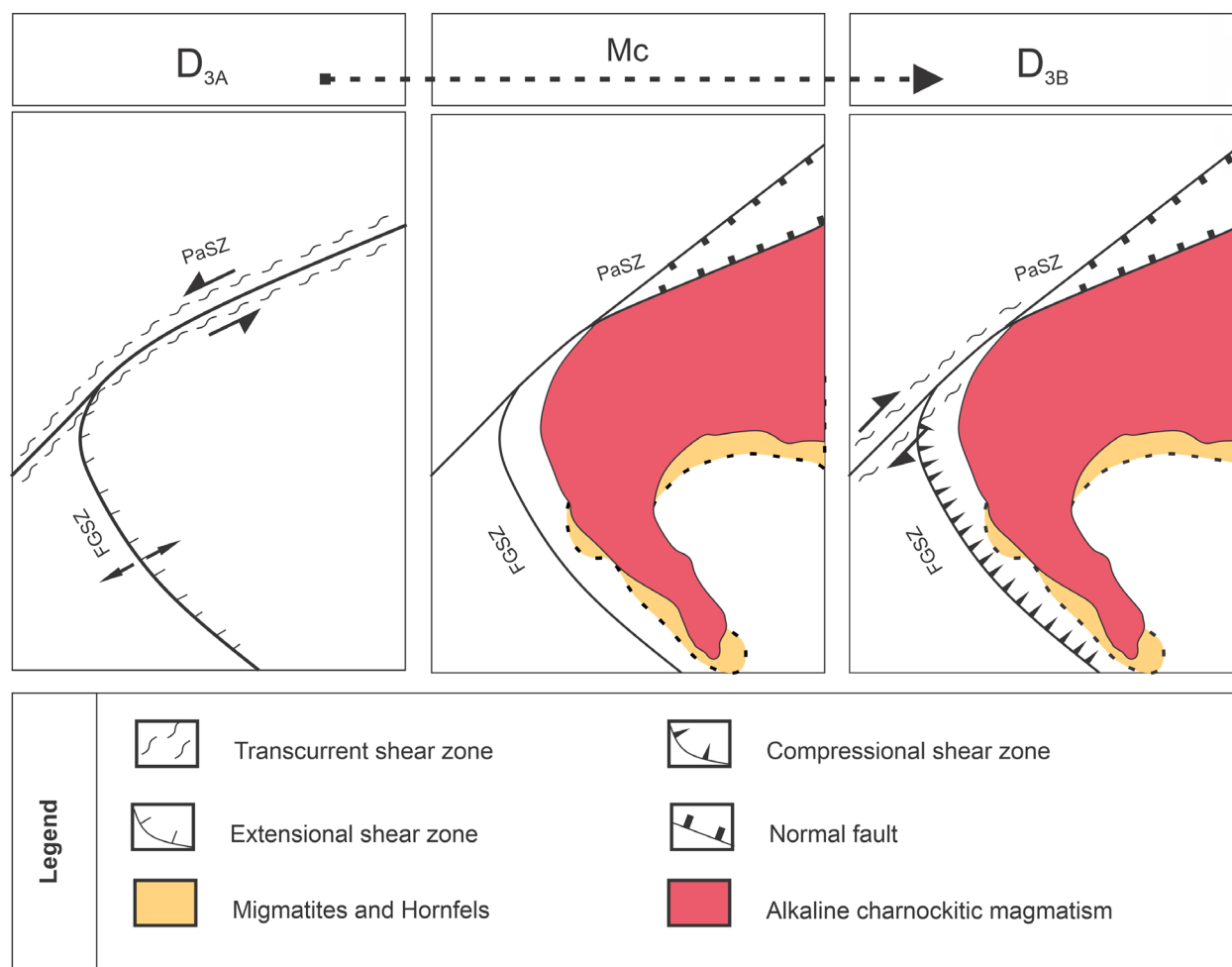


Figure 16. Suggested tectonic evolution. The process begins with an anti-clockwise extensional movement of the PaSZ coupled with a normal extensional movement of the FGSZ, allowing the emplacement of Umarizal magma and provoking contact metamorphism (Mc) of the host Jucurutu Formation rocks (the D_{3A} event). In the next stage (D_{3B}), tectonic inversion occurs, when the PaSZ acquires clockwise kinematics and the FGSZ functioned as thrust fault.

grounds (Galindo 1993). In addition, this author presents data showing whole-rock geochemical similarity between these two granitoids, especially when comparing parameters such as oxygen fugacity, SiO₂ concentration, #Fe, and mineral-chemical types.

The geochronological results reported herein, and the aforementioned interpretations are both coherent with the intrusion of the Umarizal body into the Tourão-Caraúbas granitoid, as observed through dykes and interdigitated or sinuous contacts (Fig. 6B). These kinds of features suggest that the Tourão-Caraúbas magma was still hot enough to allow the capture of crystals or magma mixture. Although the second hypothesis is incompatible with the age of the analyzed neosome, such a possibility cannot be ruled out considering the regional context.

In a broader aspect, the reported time range (600-580 Ma) encompasses other Ediacaran granitoids intrusive into the Seridó Group and commonly associated with HT/LP metamorphism (Fig. 17), such as the Acari Granite (Itaporanga type; 577 ± 5 Ma — Archanjo *et al.* 2013; 585 ± 6 Ma — Souza *et al.* 2019), the Totoró Gabbro-Norite and granite (Shoshonite and Itaporanga types, with the respective ages of 595 ± 3 and 591 ± 4 Ma; Archanjo *et al.* 2013), and the Catingueira pluton along the Patos Shear Zone (Alkaline type; 573 ± 14 Ma; Souza *et al.* 2017a). These ages match a mineral + whole rock Sm-Nd isochron for peraluminous neosomes (575 ± 2 Ma

— Souza *et al.* 2006; 590 ± 3 Ma — Souza *et al.* 2019), and ages for the Japi Alkaline Granite (599 ± 3 Ma; Souza *et al.* 2016) and Gameleiras -and Serrinha plutons (573 ± 7 — 576 ± 3 Ma; Galindo *et al.* 2005) to the east of the Picuí — João Câmara Lineament. The presence of all those bodies over an expressive surface area strongly suggests a prominent regional thermal anomaly in this part of the Borborema Province in the late Ediacaran period (600-559 Ma).

Lima *et al.* (1989) proposed temperatures of intrusion in the range 580-700°C and pressures of 4-6 kbar for the region to the east of the Umarizal Granite based on thermobarometric data in pyroxene-hornfels from the contact of Seridó Formation micaschist with the Totoró Gabbro-Norite. Such results are consistent with the emplacement of Ediacaran plutons slightly preceding a regional HT / LP transpressional event around 575 Ma in northeast Brazil and west Africa (Archanjo *et al.* 2013).

When considering the geological provinces in West Africa as continuous with those of the Borborema province during the Brazilian orogen, it is worth mentioning that a large number of African Ediacaran plutons produced metamorphic aureoles on hosting supracrustal rocks, with geologic, petrographic, metamorphic, and geochronological characteristics akin to those reported here for the Umarizal region. Oyawoye (1962) and Ferré *et al.* (1997) described gradual contacts between fayalite-quartz monzonite and biotite-hornblende granite at Bauchi and Rahaman (Nigeria) with zircon U-Pb ages of 638-580 Ma for orthopyroxene-bearing granites (Tubosun *et al.* 1984, Dada *et al.* 1989) and migmatization of 581 ± 10 Ma (Ferré *et al.* 1996). Dada *et al.* (1995) distinguished two charnockite granitoid groups:

- calc-alkaline granodioritic association at Toro;
- sub-alkaline monzonitic association at Bauchi, Saminaka and Dindima regions.

Hornblende corona around pyroxenes (Ferré *et al.* 1997) and hornblende + quartz symplectite (Ademeso and Olaleye 2014) were also described. Following Oyawoye (1962), the migmatite zone surrounds the granites and charnockites are biotite-garnet-bearing gneiss, banded gneiss, calc-silicate gneiss, and agmatitic gneiss. Ferré *et al.* (1997) interpreted that strike-slip shear zones were active during and slightly after the emplacement of the Nigerian calc-alkaline charnockite pluton of Rahaman.

Considering the whole context described above, the peak of heat flow during the Ediacaran could have triggered a relevant thermal and tectono-metamorphic input for the thermo-tectonic evolution of both the Borborema Province and the geological blocks of NW Africa. Granitic systems on this scale would significantly change the rheological and mineralogical parameters leading to a prominent modification of the continental geothermal gradients (Paterson and Fowler 1993a, Ingram and Hutton 1994, Brown and Solar 1999, Neves *et al.* 2000).

Mechanism of magma emplacement

During the emplacement of syntectonic magmas, features such as foliation, lineation, metamorphic layering, and the shear

Table 1. Comparative geochemistry of the Umarizal and Tourão-Caraúbas granitoids. Data compiled from Galindo (1993), Campos *et al.* (2016), and this work.

	Umarizal granite	Tourão-Caraúbas granite
T _{Zr} (°C)	882 ± 31 ¹	761 ± 34 ¹
P (kbar)	≤ 4.5 ³	5.5 ± 0.5 ²
fO ₂	QFM ³	QFM + 0.4 to QFM + 0.7 ²
U-Pb age (Ma)	563.7 ± 6.2; 587.2 ± 2.3 ³	589.3 ± 4.4 ³
SiO ₂ (wt. %)	63.3 to 75.0 ¹	63.9 to 78.5 ¹
Magmatic series	Transitional calc-alkaline to alkaline ¹	Calc-alkaline ¹
#Fe	0.88 to 0.96 ¹	0.81 to 0.92 ¹
Na ₂ O + K ₂ O (wt. %)	8.62 to 10.36 ¹	7.98 to 9.26 ¹
Rb (ppm)	99 to 162 ¹	163 to 376 ¹
Sr (ppm)	107 to 242 ¹	110 to 380 ¹
Zr (ppm)	337 to 962 ¹	97 to 438 ¹
La _N /Yb _N	12.5 to 61.8 ¹	20.3 to 101.7 ¹
Yb _(N)	10.7 to 23.7 ¹	4.1 to 19.1 ¹
Amphibole	Transitional hornblende to Pargasite ¹	Pargasite ²
Biotite	Annite ¹ [Fe ²⁺ /(Fe ²⁺ +Mg)] = 0.8 to 0.9	Annite ² [Fe ²⁺ /(Fe ²⁺ +Mg)] = 0.6 to 0.7
Plagioclase	Oligoclase (An ₂₁₋₂₂) ¹	Oligoclase (An _{19,25}) ¹

¹Galindo (1993); ²Campos *et al.* (2016); ³This work; T_{Zr}: zircon saturation temperature based on Gervasoni *et al.* (2016); fO₂: oxygen fugacity; QFM: Quartz-Fayalite-Magnetite buffer; #Fe: FeO_T/(MgO+FeO_T), La and Yb Chondrite-normalizing values from Evensen *et al.* (1978).

band can develop over the country rocks, as well as composite S/C magmatic fabric, as underlined by Blumenfeld and Bouchez (1988), Benn and Allard (1989), Paterson *et al.* (1989), and Schulmann *et al.* (1996). The absence of these features demonstrates that no expressive ductile deformational episode (here named D₃) has acted synchronously during emplacement of the Umarizal pluton. Therefore, it is concluded that the ductile fabrics observed on the Jucurutu Formation host rocks were formed shortly before the magma emplacement.

According to Galindo (1993), the granitic magma that formed the Umarizal pluton was originated by partial melting of the lower granulitic crust and rose through ductile shear zones (the deformation episode D_{3A}). Afterward, Archanjo *et al.* (1998) suggested a contemporaneity of the pluton with plastic deformation of the country rocks under metamorphic conditions equivalent to the upper amphibolite facies and syn-tectonically to the reactivation of the FGSZ. Through magnetic susceptibility anisotropy data, Archanjo *et al.* (1998) suggested a diapiric emplacement for the Umarizal magma, controlled by the shear zone. On the other hand, McReath *et al.* (2002) suggested a lacolithic geometry having a feeding system underneath the Jucurutu Formation rocks.

Considering the geobarometric conditions operating during magma rising, McReath *et al.* (2002) advocated that the beginning of crystallization of the magma, which produced the Umarizal pluton, occurred at 7-8 kbar, formed the association

fayalite + quartz or orthopyroxene. They also reported the crystallization of amphibole at slightly lower pressures (4.7-5.7 kbar), by using the Al-in hornblende geobarometer. These pressure estimates are within those determined by Campos *et al.* (2016), in the range 4.8-6.0 kbar for the Tourão-Caraúbas granite that occurs in the same region. Therefore, these pressure ranges do not satisfy the barometric conditions for mineral associations present in the contact aureole of the Umarizal pluton. Based on the presence of andalusite / sillimanite in the contact aureole, the pressure in the region should not exceed ~4.5 kbar for magma emplacement, with the higher pressures possibly corresponding to earlier mineral crystallization phases (Holdaway 1971, Winter 2013).

Archanjo *et al.* (1998) explained the transport and emplacement model for the Umarizal pluton during extensional movements along the FGSZ that allowed migration of magma through a flat structure in the lower crust. Following these authors, the extending shape to the east in the northern portion of the Umarizal body occurs by dextral kinematics control in the PaSZ. However, as considered in this work, the dextral component in the PaSZ would have occurred at a later stage to the extensional movement. Furthermore, in the hypothesis of dextral and extensional kinematics occurring simultaneously in PaSZ and FGSZ, sinistral component would affect the magmatic fabric and the shape of the pluton, which was not observed.

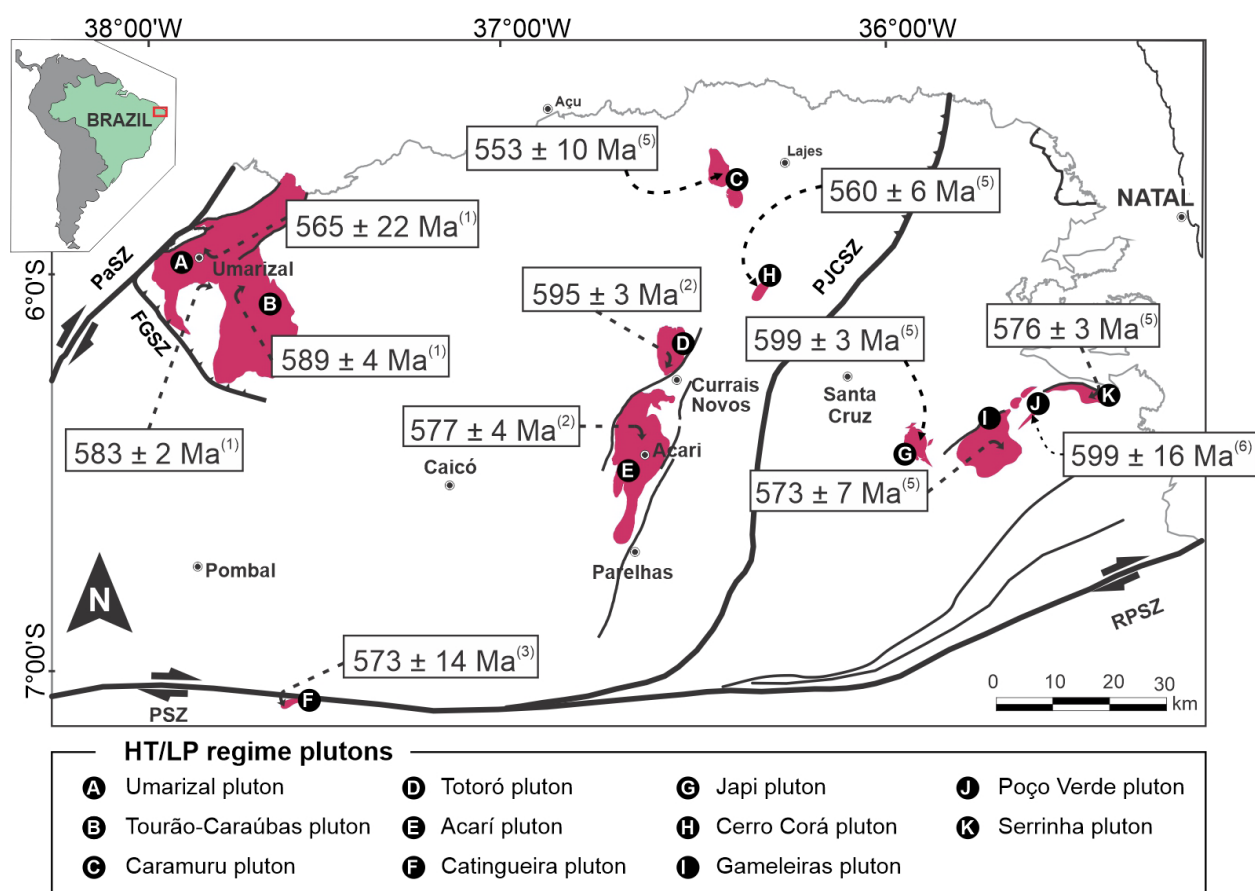


Figure 17. Schematic geological map of the Rio Grande do Norte Domain showing the main Ediacaran magmatic bodies emplaced under high-temperature / low-pressure (HT/LP) regime and associated shear zones. Abbreviations: PaSZ Portalegre shear zone, FGSZ Frutuoso Gomes shear zone, PSZ Patos shear zone, RPSZ Remígio-Pocinhos shear zone, PJCSZ Picuí - João Câmara shear zone. Reference for U-Pb geochronology dates: (1) this work; (2) Archanjo *et al.* (2013); (3) Souza *et al.* (2017a); (4) Souza *et al.* (2006); (5) Souza *et al.* (2016), (6) Dantas (1996).

To explain granitic magma ascent, we will follow the methodology of Brown (1994), which is divided into three stages:

1. segregation;
2. transport;
3. emplacement.

The first stage corresponds to the production of magma by partial melting and its separation from the source region. Step (2) refers to any models allowing magma to rise through the crust. The third step corresponds to the mechanisms that contribute to the emplacement and accommodation of magma at shallower depths. The mineralogical associations generated during the contact metamorphism of the host rocks allow us to assume a transition region between the middle and upper crusts for the Umarizal pluton emplacement, a situation akin to the one described by Paterson and Fowler (1993b) and Weinberg (1996).

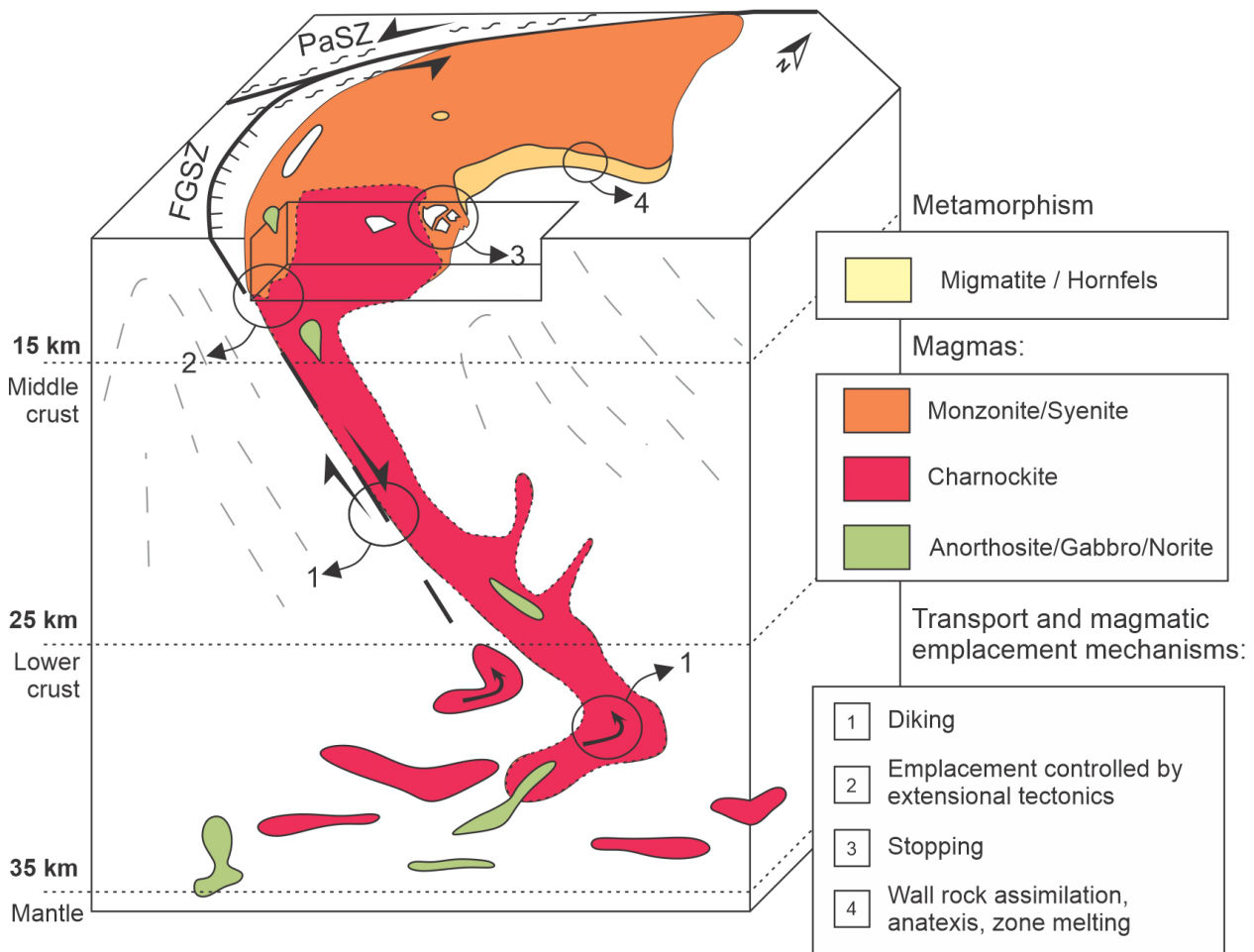
Following the proposal of Paterson *et al.* (1991), the thermal aureole around the Umarizal body can encompass four main mechanisms:

- stopping;
- assimilation and / or anatexis of the country rocks;
- magma accommodation within spaces generated by an extensional tectonic;
- diking.

Among the features corroborating these processes, we outline the following:

- the shape of igneous bodies that is usually rounded and unoriented when far from shear zones, but parallelized and more elongated when approaching these structures;
- the presence of hectometric or kilometeric xenoliths and magmatic breccias (stopping) close to the contact of the igneous body with the host rocks;
- following Frost and Frost (2011), the stages of crustal assimilation during magmatic evolution associated to mafic magmas are quite characteristic during the ascension of opx-bearing granitic alkaline magmas;
- the occurrence of migmatitic features inside the metamorphic aureoles contouring the pluton;
- the absence of compressional ductile structures concomitant to the intrusive body in the country rocks;
- the occurrence of normal / extensional oblique structures in the FGSZ;
- the sinistral strike-slip structures preceding the dextral kinematics in the PaSZ.

Figure 18 illustrates the model proposed for the study area by considering the above arguments. The emplacement system that best fits the geological and structural characteristics of the Umarizal pluton is the one involving laccoliths



FGSZ: Frutuoso Gomes Shear Zone; PaSZ: Portalegre Shear Zone.

Figure 18. Block-diagram illustrating the successive stages of segregation, transport, and emplacement of the Umarizal magmas, based on Paterson *et al.* (1991).

/ lopoliths and sills / dykes as proposed by Rubin (1993). According to the model, both transport and magma emplacements are controlled by space opened during extensional tectonics (Castro 1987, Hutton *et al.* 1990, Rubin 1993). Firstly, basaltic magmas, represented by gabbros and norites, originated in the upper mantle and granitic magmas derived from the melting of Paleoproterozoic infracrust (Nd T_{DM} model age of 2.16 Ga, $\epsilon_{Nd}(t)$ of -16.4; Sá *et al.* 2014) are positioned in magmatic chambers at middle crustal depth. Succeeding the thermal effect provoked by emplacement and cooling of magmas, tectonic reversal occurs, leading to a westward movement of the eastern block and the consequent behavior of the PaSZ and FGSZ with dextral strike-slip and thrusting kinematics, respectively. An alternative emplacement model involves lowering the floor of the magma chamber, with the magmatic intrusion taking advantage of the shear zones and basement/supracrustal contact, and then migrating northwards. In this case, it is possible to infer that the Umarizal granite is a thin body and its country rocks are exposed in the southwestern portion because of anti-formal folding and subsequent erosion of the granite upper portion.

CONCLUSIONS

The data presented allow us to suggest the following conclusions:

- PaSZ and FGSZ were initially evolved, respectively, as sinistral transcurrent and extensional normal, reversing in a second moment to dextral transcurrent and thrusting;
- This initial episode led to the opening of spaces that served as magma conduits (mainly by dike) and the formation of lopolith / lopolith magma chamber;
- U-Pb zircon dating of neosome from migmatized hornfels and from the Tourão and Caraúbas granites provided the ages of 580 ± 4 Ma, 589 ± 4 Ma, and 563 ± 6 Ma, respectively;
- The emplacement of the Umarizal pluton at upper crustal level (4-5 kbar) and high temperatures ($\sim 800^\circ\text{C}$) generated contact aureole of up to 2 km width, with stabilization of

metamorphic parageneses involving andalusite, sillimanite, scapolite, garnet, and forsterite within metasedimentary host rocks and xenoliths;

- It is suggested that the emplacement of the Umarizal and Tourão-Caraúbas granites and the subsequent thermal effect have taken place within a time of ~ 26 Ma (589-563 Ma);
- Since plutonic bodies emplaced at high temperatures in a low-pressure environment also occur in eastern Africa and share similar geological, structural, geochemical, and geochronological characteristics with the Borborema Province, it is conceivable to correlate the charnockitic magmatism to a more widespread episode of thermal input in both regions in the Late Ediacaran.

ACKNOWLEDGMENTS

The authors acknowledge the Programa de Pós-Graduação em Geodinâmica e Geofísica (Geodynamics and Geophysics Post-Graduate Program), Universidade Federal do Rio Grande do Norte (PPGG-UFRN), Geosciences Institute of the Universidade Estadual de Campinas (IG-Unicamp) and the Conselho Nacional de Desenvolvimento Científico e Tecnológico (National Council for Scientific and Technological Development – CNPq projects 449616/2014-2 and 305661/2016-7, coordinator Z.S. Souza) for financial support for data acquisition. S.N. Valcácio thanks Coordenação de Aperfeiçoamento de Pessoal de Nível Superior (Coordination for the Improvement of Higher Education Personnel – CAPES) for a Ph. D. scholarship. Suggestions by two anonymous reviewers helped to improve the earlier version of the manuscript and are deeply appreciated.

APPENDIX

This paper has a Supplementary data table with all available zircon U-Th-Pb isotopic analysis results reported along with the text.

ARTICLE INFORMATION

Manuscript ID: 20200129. Received on: 11 DEC 2020. Approved on: 02 FEB 2022.

How to cite this article: Valcácio S.M., Souza Z.S., Oliveira E.P. U-Pb zircon age of Ediacaran Umarizal Granite Suite and emplacement mechanism with high-T hornfels generation in Jucurutu Formation, Borborema Province, NE, Brazil. *Brazilian Journal of Geology*, 52(1):e20200129, 2022. <https://doi.org/10.1590/2317-488920220200129>.

S.V. wrote the first draft of the manuscript and prepared all figures presented; Z.S. provided resources, guidance, and improved the manuscript through corrections and suggestions. E.O. provided geochronological data analysis and revised and improved the manuscript.

Competing interests: The authors declare no competing interests.

REFERENCES

- Ademeso O.A., Olaley B.M. 2014. Physicomechanical Characteristics of Charnokitic Rock of Akure, Southwest Nigeria. *General Scientific Researches*, 2(1):31-37.
- Almeida F.F.M., Hasui Y., Brito Neves B.B., Fuck R.A. 1981. Brazilian structural provinces: an introduction. *Earth Science Review*, 17(1-2):1-29. [https://doi.org/10.1016/0012-8252\(81\)90003-9](https://doi.org/10.1016/0012-8252(81)90003-9)
- Almeida K.M.F., Jenkins D.M. 2017. Stability field of the Cl-rich scapolite marialiate. *American Mineralogist*, 102(12):2484-2493. <https://doi.org/10.2138/am-2017-6132>
- Angelim L.A.A., Nesi J.R., Torres H.H.F., Medeiros V.C., Santos C.A., Veiga Junior J.P., Mendes V.A. 2006. *Geologia e recursos minerais do Estado do Rio Grande do Norte*. Escala 1:500.000. Texto explicativo dos mapas geológico e de recursos minerais do Estado do Rio Grande do Norte. Recife: CPRM/SEDEC-RN/FAPERNA, 119 p.
- Archanjo C.J., Macedo J.W.P., Galindo A.C., Araújo M.G.S. 1998. Brasiliano Crustal extension and emplacement fabrics of the magerite-charnockite pluton of Umarizal, North-east Brazil. *Precambrian Research*, 87(1-2):19-32. [https://doi.org/10.1016/S0301-9268\(97\)00050-8](https://doi.org/10.1016/S0301-9268(97)00050-8)

- Archanjo C.J., Viegas L.G.F., Hollanda M.H.B.M., Souza L.C., Liu D. 2013. Timing of the HT/LP transpression in the Neoproterozoic Seridó Belt (Borborema Province, Brazil): Constraints from UPb (SHRIMP) geochronology and implications for the connections between NE Brazil and West Africa. *Gondwana Research*, **23**(2):701-714. <https://doi.org/10.1016/j.gr.2012.05.005>
- Barton M.D., Staude J.M., Snow E.A., Johnson D.A. 1991. Aureole systematics. In: Kerrick D.M. (ed.). *Contact metamorphism*. Chelsea: Mineralogical Society of America, p. 723-847.
- Benn K., Allard B. 1989. Preferred mineral orientations related to magmatic flow in ophiolite layered gabbros. *Journal of Petrology*, **30**(4):925-946. <https://doi.org/10.1093/petrology/30.4.925>
- Blumenfeld P., Bouchez J.-L. 1988. Shear criteria in granite and migmatite deformed in the magmatic and solid states. *Journal of Structural Geology*, **10**(4):361-372. [https://doi.org/10.1016/0191-8141\(88\)90014-4](https://doi.org/10.1016/0191-8141(88)90014-4)
- Brito Neves B.B., Santos E.J., Van Schmus W.R. 2000. Tectonic history of the Borborema Province, Northeastern Brazil. In: Cordani U.G., Milani E.J., Thomaz Filho A., Campos D.A. (eds.). *Tectonic evolution of South America*. 31st International Geological Congress. Rio de Janeiro, p. 51-182.
- Brown M. 1994. The generation, segregation, ascent and emplacement of granite magma: the migmatite-to-crustally-derived granite connection in thickened orogens. *Earth-Science Reviews*, **36**(1-2):83-130. [https://doi.org/10.1016/0012-8252\(94\)90009-4](https://doi.org/10.1016/0012-8252(94)90009-4)
- Brown M., Solar G.S. 1998. Granite ascent and emplacement during contractional deformation in convergent orogens. *Journal of Structural Geology*, **20**(9-10):1365-1393. [https://doi.org/10.1016/S0191-8141\(98\)00074-1](https://doi.org/10.1016/S0191-8141(98)00074-1)
- Brown M., Solar G.S. 1999. The mechanism of ascent and emplacement of granite magma during transpression: a syntectonic granite paradigm. *Tectonophysics*, **312**(1):1-33. [https://doi.org/10.1016/S0040-1951\(99\)00169-9](https://doi.org/10.1016/S0040-1951(99)00169-9)
- Bucher K., Frost B.R. 2006. Fluid transfer in high-grade metamorphic terrains intruded by anorogenic granites: The Thor range, Antarctica. *Journal of Petrology*, **47**(3):567-593. <https://doi.org/10.1093/petrology/egi086>
- Caby R., Sial A.N., Ferreira V.P. 2009. High-pressure thermal aureoles around two Neoproterozoic synorogenic magmatic epidote-bearing granitoids, Northeastern Brazil. *Journal of South American Earth Sciences*, **27**(2-3):184-196. <https://doi.org/10.1016%2Fj.jsames.2008.09.005>
- Campos B.C.S., Vilva F.C.J., Nascimento M.A.L., Galindo A.C. 2016. Crystallization conditions of porphyritic high-K calc-alkaline granitoids in the extreme northeastern Borborema Province, NE Brazil, and geodynamic implications. *Journal of South American Earth Sciences*, **70**:224-236. <https://doi.org/10.1016/j.jsames.2016.05.010>
- Castro A. 1987. On granitoid emplacement and related structures. A review. *Geologische Rundschau*, **76**:101-124. <https://doi.org/10.1007/BF01820576>
- Chagas C.F., Souza Z.S., Moreira J.A.D.M. 2018. Auréola termal provocada pela intrusão do pluton Totoró em micaxistos do Grupo Seridó, Ediacarano da Província Borborema, NE do Brasil. *Geologia USP. Série Científica*, **18**(3):117-139. <https://doi.org/10.11606/issn.2316-9095.v18-125724>
- Cunha J.A.P., Souza Z.S., Moreira J.A.D.M., Valcácio S.N. 2018. Mecanismo de colocação e auréola termal provocada pelo plúton Ediacarano Catingueira, Província Borborema, Nordeste do Brasil. *Geologia USP. Série Científica*, **18**(4):209-226. <https://doi.org/10.11606/issn.2316-9095.v18-143141>
- Dada S.S., Briquieu L., Harns U., Lancelot J.R., Matheis G. 1995. Charnockitic and monzonitic Pan-African series from north-central Nigeria: Trace-element and Nd, Sr, Pb isotope constraints on their petrogenesis. *Chemical Geology*, **124**(3-4):233-252. [https://doi.org/10.1016/0009-2541\(95\)00010-J](https://doi.org/10.1016/0009-2541(95)00010-J)
- Dada S.S., Lancelot J.R., Briquieu L. 1989. Age and origin of the annular charnockitic complex at Toro, Northern Nigeria: U-Pb and Rb-Sr evidence. *Journal of African Earth Sciences*, **9**(2):227-234. [https://doi.org/10.1016/0899-5362\(89\)90066-3](https://doi.org/10.1016/0899-5362(89)90066-3)
- Dantas E.L. 1996. *Geocronologia U-Pb e Sm-Nd de terrenos arqueanos e paleoproterozóicos do Maciço Caldas Brandão, NE do Brasil*. PhD Thesis, Universidade Estadual Paulista "Júlio de Mesquita Filho", Rio Claro, 208 p.
- Davidson J.P., Morgan D.J., Charlie B.L.A., Harlou R., Hora J.M. 2007. Microsampling and isotopic analysis of igneous rocks: Implications for the study of magmatic systems. *Annual Reviews of Earth and Planetary Science*, **35**:273-311. <https://doi.org/10.1146/annurev.earth.35.031306.140211>
- Evensen N.M., Hamilton P.J., O'niions R.K. 1978. Rare-Earth abundances in chondritic meteorites. *Geochimica et Cosmochimica Acta*, **42**(8):1199-1212. [https://doi.org/10.1016/0016-7037\(78\)90114-X](https://doi.org/10.1016/0016-7037(78)90114-X)
- Ferré E., Déléris J., Bouchez J.L., Lar A.U., Peucat J.J. 1996. The Pan-African reactivation of Eburnean and Archaean provinces in Nigeria: Structural and isotopic data. *Journal of the Geological Society*, **153**(5):719-728. <https://doi.org/10.1144/gsjgs.153.5.0719>
- Ferré E., Gleizes G., Djouadi M.T., Bouchez J.L., Ugodulunwa F.X.O. 1997. Drainage and emplacement of magmas along an inclined transcurrent shear zone: Petrophysical evidence from a granite-charnockite pluton (Rahama, Nigeria). In: Bouchez J.L., Hutton D.H.W., Stephens W.E. (eds.). *Granite: from segregation of melts to emplacement fabrics*. Dordrecht: Kluwer, 253-273.
- Frost B.R., Frost C.D. 2008. On charnockites. *Gondwana Research*, **13**:30-44. <https://doi.org/10.1016/j.gr.2007.07.006>
- Frost C.D., Frost B.R. 2011. On ferroan (A-type) granitoids: their compositional variability and modes of origin. *Journal of Petrology*, **52**(1):39-53. <https://doi.org/10.1093/petrology/egq070>
- Galindo A.C. 1993. *Petrologia dos Granitóides Brasileiros da Região de Caraiúbas - Umarizal, oeste do Rio Grande do Norte*. PhD Thesis, Universidade Federal do Pará, Belém, 319 p.
- Galindo A.C., Dall'Agnol R., McReath I., Lafon J.M., Teixeira N. 1995. Evolution of Brasileiro-age granitoid types in a shear-zone environment, Umarizal-Caraubas region, Rio Grande do Norte, northeast Brazil. *Journal of South American Earth Sciences*, **8**(1):79-95. [https://doi.org/10.1016/0895-9811\(94\)00043-2](https://doi.org/10.1016/0895-9811(94)00043-2)
- Galindo A.C., Souza Z.S., Dantas E.L., Antunes A.F., Dias L.G.S., Silva F.C., Laux J.H. 2005. Geocronologia U-Pb de granitóides tipo Itaporanga (Monte das Gameleiras e Serrinha), Maciço São José do Campestre, NE do Brasil. In: Simpósio de Geologia do Nordeste, 20., 2005, Recife. *Proceedings*, p. 150-152.
- Gervasoni F., Klemme S., Rocha-Junior E.R.V., Berndt J. 2016. Zircon saturation in silicate melts: a new and improved model for aluminous and alkaline melts. *Contributions to Mineralogy and Petrology*, **171**:21. <https://doi.org/10.1007/s00410-016-1227-y>
- Hackspacher P.C., Legrand J.M. 1989. Microstructural and metamorphic evolution of the Portalegre shear zone, Northeastern Brazil. *Revista Brasileira de Geociências*, **19**(1):63-75.
- Holdaway M.J. 1971. Stability of andalusite and the aluminosilicate phase diagram. *American Journal of Science*, **271**(2):97-131. <https://doi.org/10.2475/ajs.271.2.97>
- Hutton D.H.W., Dempster T.J., Brown P.E., Becker S.D. 1990. A new mechanism of granite emplacement: intrusion in active extensional shear zones. *Nature*, **343**:452-455. <https://doi.org/10.1038/343452a0>
- Ingram G.M., Hutton D.H.W. 1994. The Great Tonalite Sill: Emplacement into a contractional shear zone and implications for Late Cretaceous to early Eocene tectonics in southeastern Alaska and British Columbia. *Geological Society of America Bulletin*, **106**(5):715-728. [https://doi.org/10.1130/0016-7606\(1994\)106%3C0715:TGTSEI%3E2.3.CO;2](https://doi.org/10.1130/0016-7606(1994)106%3C0715:TGTSEI%3E2.3.CO;2)
- Jardim de Sá E.F. 1984. A evolução proterozóica da Província Borborema. In: Simpósio de Geologia do Nordeste, 11., 1984, João Pessoa. *Proceedings*, p. 297-316.
- Jardim de Sá E.F. 1994. *A Faixa Seridó (Província Borborema, NE do Brasil) e o seu Significado Geodinâmico na Cadeia Brasileira/Pan-Africana*. PhD Thesis, Universidade de Brasília, Brasília, 804 p.
- Kase H.R., Metz P. 1980. Experimental investigation of the metamorphism of siliceous dolomites; IV, Equilibrium data for the reaction: 1dolomite + 3diopside = 2forsterite + 4calcite + 2CO₂. *Contributions to Mineralogy and Petrology*, **73**:151-159. <https://doi.org/10.1007/BF00371390>
- Lima E.S., Pessoa R.J., Accioli A.C. 1989. O metamorfismo de contato causado pelo gabronorito de Totoró, Currais Novos, Rio Grande do Norte, Nordeste Brasileiro. *Revista Brasileira de Geociências*, **19**(3):323-329.
- McReath I., Galindo A.C., Dall'Agnol R. 2002. The Umarizal Igneous Association, Borborema Province, NE Brazil: Implications for the Genesis of A-Type Granites. *Gondwana Research*, **5**(2):339-353. [https://doi.org/10.1016/S1342-937X\(05\)70727-9](https://doi.org/10.1016/S1342-937X(05)70727-9)
- Moecher D.P., Essene E.J. 1990. Phase equilibria for calcic scapolite, and implications of variable Al-Si disorder for P-T, T-XCO₂, and a-X relations. *Journal of Petrology*, **31**(5):997-1024. <https://doi.org/10.1093/petrology/31.5.997>
- Morais Neto J.M. 1987. *Mapeamento geológico da zona de cisalhamento de portalegre (ZCP) e encaixantes, numa área entre Caraiúbas, Apodi e Umarizal (RN)*. Monografia, Universidade Federal do Rio Grande do Norte, Natal, 224 p.

- Nascimento M.A.L., Antunes A.F., Galindo A.C., Jardim de Sá E.F., Souza Z.S. 2000. Geochemical signatures of the Brasiliano-age plutonism in the Seridó belt, Northeastern Borborema Province. *Revista Brasileira de Geociências*, **30**(1):161-164.
- Nascimento M.A.L., Galindo A.C., Medeiros V.C. 2015. Ediacaran to Cambrian magmatic suites in the Rio Grande do Norte domain, extreme Northeastern Borborema Province (NE of Brazil): Current knowledge. *Journal of South American Earth Sciences*, **58**:281-299. <https://doi.org/10.1016/j.jsames.2014.09.008>
- Nascimento M.A.L., Medeiros V.C., Galindo A.C. 2008. Magmatismo Ediacarano a Cambriano no Domínio Rio Grande do Norte, Província Borborema, NE do Brasil. *Estudos Geológicos*, **18**:4-25.
- Navarro M.S., Tonetto E.M., Oliveira E.P. 2017. Peixe zircon: new Brazilian reference material for U-Pb geochronology by LA-SF-ICP-MS. In: Goldschmidt, 2017. *Abstract*, 1 p.
- Neves S.P., Vauchez A., Feraud G. 2000. Tectono-thermal evolution, magma emplacement, and shear zone development in the Caruaru area (Borborema Province, NE Brazil). *Precambrian Research*, **99**(1-2):1-32. [https://doi.org/10.1016/S0301-9268\(99\)00026-1](https://doi.org/10.1016/S0301-9268(99)00026-1)
- Newton R.C., Goldsmith J.R. 1976. Stability of the end-member scapolites: $3\text{NaAlSi}_3\text{O}_8 \cdot \text{NaCl}$, $3\text{CaAl}_2\text{Si}_2\text{O}_8 \cdot \text{CaCO}_3$, $3\text{CaAl}_2\text{Si}_2\text{O}_8 \cdot \text{CaSO}_4$. *Zeitschrift für Kristallographie – Crystalline Materials*, **143**:333-353. <https://doi.org/10.1524/zkri.1976.143.jg.333>
- Oliveira R.G., Medeiros W.E. 2018. Deep crustal framework of the Borborema Province, NE Brazil, derived from gravity and magnetic data. *Precambrian Research*, **315**:45-65. <https://doi.org/10.1016/j.precamres.2018.07.004>
- Oyawoye M.O. 1962. The petrology of the district around Bauchi, Northern Nigeria. *Journal of Geology*, **70**(5):604-615. <https://doi.org/10.1086/626855>
- Paterson S.R., Fowler T.K. 1993a. Extensional pluton-emplacement models: Do they work for large plutonic complexes? *Geology*, **21**(9):781-784. [https://doi.org/10.1130/0091-7613\(1993\)021%3C0781:EPMDT%3E2.3.CO;2](https://doi.org/10.1130/0091-7613(1993)021%3C0781:EPMDT%3E2.3.CO;2)
- Paterson S.R., Fowler T.K. 1993b. Re-examining pluton emplacement processes. *Journal of Structural Geology*, **15**(2):191-206. [https://doi.org/10.1016/0191-8141\(93\)90095-R](https://doi.org/10.1016/0191-8141(93)90095-R)
- Paterson S.R., Vernon R.H., Fowler T.K. 1991. Aureole tectonics. In: Kerrick D.M. (ed.). *Contact Metamorphism. Reviews in Mineralogy*, **26**:673-722.
- Paterson S.R., Vernon R.H., Tobisch O. T. 1989. A review of criteria for the identification of magmatic and tectonic foliations in granitoids. *Journal of Structural Geology*, **11**(3):349-363. [https://doi.org/10.1016/0191-8141\(89\)90074-6](https://doi.org/10.1016/0191-8141(89)90074-6)
- Pattison D.R.M. 2001. Instability of Al_2SiO_5 "triple-point" assemblages in muscovite+biotite+quartz-bearing metapelites, with implications. *American Mineralogist*, **86**(11-12):1414-1422. <https://doi.org/10.2138/am-2001-11-1210>
- Pattison D.R.M., Spear F.S., Debuhr C.L., Cheney J.T., Guidotti C.V. 2002. Thermodynamic modelling of the reaction muscovite + cordierite \rightarrow Al_2SiO_5 + biotite + quartz + H_2O : constraints from natural assemblages and implications for the metapelitic petrogenetic grid. *Journal of Metamorphic Geology*, **20**(1):99-118. <https://doi.org/10.1046/j.0263-4929.2001.356.356.x>
- Rubin A.M. 1993. Dikes vs. diapirs in viscoelastic rock. *Earth and Planetary Science Letters*, **117**(3-4):653-670. [https://doi.org/10.1016/0012-821X\(93\)90109-M](https://doi.org/10.1016/0012-821X(93)90109-M)
- Sá J.M., Galindo A.C., Legrand J.M., Souza L.C., Maia H.N. 2014. Os granitos ediacaranos no contexto dos terrenos Jaguaribeano e Rio Piranhas-Seridó no oeste do RN, Província Borborema. *Estudos Geológicos*, **24**(1):3-22. <https://doi.org/10.18190/1980-8208/estudosgeologicos.v24n1p3-22>
- Santos E.J., Brito Neves B.B., Van Schmus W.R., Oliveira R.G., Medeiros V.C. 2000. An overall view on the displaced terrane arrangement of the Borborema Province, NE Brazil. In: International Geological Congress, General Symposia, Tectonic Evolution of South American Platform, 31, 2000, Rio de Janeiro. *Proceedings*, p. 5-9.
- Santos E.J., Medeiros V.C. 1999. Constraints from granitic plutonism on Proterozoic crustal growth of the Transverse Zone, Borborema Province, NE-Brazil. *Revista Brasileira de Geociências*, **29**(1):73-84.
- Schulmann K., Mlčoch B., Melka R. 1996. High-temperature microstructures and rheology of deformed granite, Erzgebirge, Bohemian Massif. *Journal of Structural Geology*, **18**(6):719-733. [https://doi.org/10.1016/S0191-8141\(96\)80007-1](https://doi.org/10.1016/S0191-8141(96)80007-1)
- Sial A.N. 1989. *Petrologia, geoquímica de elementos maiores, traços, terras raras e isótopos (Sr, O, H, S) nos batólitos da Meruoca e Mocambo, Ceará, Nordeste do Brasil*. Thesis, Universidade Federal de Pernambuco, Recife, 228 p.
- Silva F.E., Lima A.S.S., Nobre M.L., Dantas T.B., Fontes V.C., Diniz P.N., Silva W.C.B., Souza Z.S., Souza L.C. 2015. Efeito térmico nas rochas da Formação Jucurutu no entorno da Suíte Umarizal, Sul de Umarizal (RN). In: Simpósio de Geologia do Nordeste, 26., 2015, Natal. *Proceedings*, p. 185-185.
- Souza L.C., Legrand J.M., Verkaeren J. 2007. Metamorfismo térmico nos micaxistos Seridó em torno do batólito granítico de Acari (RN), Nordeste do Brasil: Química mineral de Ilmenitas e Turmalinas. *Estudos Geológicos*, **17**:71-84.
- Souza Z.S., Kalsbeek F., Deng X.-D., Frei R., Kokfelt T.F., Dantas E.L., Li J.-W., Pimentel M.M., Galindo A.C. 2016. Generation of continental crust in the northern part of the Borborema Province, northeastern Brazil, from Archean to Neoproterozoic. *Journal of South American Earth Sciences*, **68**:68-96. <https://doi.org/10.1016/j.jsames.2015.10.006>
- Souza Z.S., Martin H., Peucat J.J., Jardim de Sá E.F., Macedo M.H.D.F. 2007. Calc-alkaline magmatism at the Archean-Proterozoic transition: the Caicó Complex basement (NE Brazil). *Journal of Petrology*, **48**(11):2149-2185. <https://doi.org/10.1093/petrology/egm055>
- Souza Z.S., Montel J.-M., Gioia S.M.L.C., Hollanda M.H.B., Nascimento M.A.L., Jardim de Sá E.F., Amaro V.E., Pimentel M.M., Lardeaux J.-M., Veschambre M. 2006. Electron microprobe dating of monazite from high-T shear zones in the São José de Campestre Massif, NE Brazil. *Gondwana Research*, **9**(4):441-455. <https://doi.org/10.1016/j.jgr.2005.11.008>
- Souza Z.S., Oliveira E.P., Cruz L.B., Vilalva F.C.J. 2019. Datação U-Pb em zircão de granito peraluminoso e granodiorito tipo Itaporanga, norte do Lineamento Patos: implicações tectônicas. In: Simpósio de Geologia do Nordeste, 28., 2018, Recife, Aracaju. *Proceedings*, p. 315-315.
- Souza Z.S., Oliveira E.P., Cunha J.A.P., Vilalva F.C.J. 2017a. Idades U-Pb do granito Catingueira e metarriolito adjacente, eventos magmáticos ediacaranos do Domínio da Zona Transversal, NE do Brasil. In: Simpósio de Geologia do Nordeste, 27., 2017, João Pessoa. *Proceedings*, p. 1-1.
- Souza Z.S., Oliveira E.P., Valcárcio S.N. 2017b. Geocronologia U-Pb de granitos da região de Umarizal NE do Brasil: Alojamento de migmatização ediacaranos durante metamorfismo de alta temperatura e baixa pressão. In: Simpósio de Geologia do Nordeste, 27., 2017, João Pessoa. *Proceedings*, p. 1-1.
- Spear F.S. 1995. *Metamorphic phase equilibria and pressure – temperature – time paths*. Mineralogical Society of America, 779 p.
- Trindade R.I.F., Dantas E.L., Babinski M., Van Schmus W.R. 1999. Short-lived granitic magmatism along shear zones: evidence from U-Pb zircon and sphene ages of Caraúbas and Tourão granites. In: South American Symposium on Isotope Geology, 2., 1999, Cordoba, Argentina. *Actas*, p. 143-144.
- Tuboson I.A., Lancelot J.R., Rahaman M.A., Ocan O. 1984. U-Pb Pan-African ages of two charnockite-granite associations from Southwestern Nigeria. *Contributions to Mineralogy and Petrology*, **88**(1-2):188-195. <https://doi.org/10.1007/BF00371422>
- Valcárcio S.N., Souza Z.S., Moreira J.A.M., Cunha J.A.P. 2017. Modelagem térmica do granito alcalino de Umarizal, Leste do RN, Província Borborema. In: Simpósio de Geologia do Nordeste, 27., 2017, João Pessoa. *Proceedings*, p. 1-1.
- Van Schmus W.R., Brito Neves B.B., Williams I.S., Hacksbacher P.C., Fetter A.H., Dantas E.L., Babinski M. 2003. The Seridó Group of NE Brazil, a late Neoproterozoic pre- to syn-collisional basin in West Gondwana: Insights from SHRIMP U-Pb detrital zircon ages and Sm-Nd crustal residence (TDM) ages. *Precambrian Research*, **127**(4):287-327. [https://doi.org/10.1016/S0301-9268\(03\)00197-9](https://doi.org/10.1016/S0301-9268(03)00197-9)
- Vauchez A., Neves S., Cabry R., Corsini M., Egydio-Silva M., Arthaud M., Amaro V.E. 1995. The Borborema shear zone system, NE Brazil. *Journal of South American Earth Sciences*, **8**(3-4):247-266. [https://doi.org/10.1016/0895-9811\(95\)00012-5](https://doi.org/10.1016/0895-9811(95)00012-5)
- Weinberg R.F. 1996. Ascent mechanism of felsic magmas: news and views. *Earth and Environmental Science Transactions of the Royal Society of Edinburgh*, **87**(4):541. <https://doi.org/10.1017/S0263593300018204>
- Wiedenbeck M.A.P.C., Alle P., Corfu F., Griffin W.L., Maier M., Oberli F.V., Roddick J.C., Spiegel W. 1995. Three natural zircon standards for U-Th-Pb, Lu-Hf, trace element and REE analyses. *Geostandards and Geoanalytical Research*, **19**(1):1-23. <https://doi.org/10.1111/j.1751-908X.1995.tb00147.x>
- Winter J.D. 2013. *Principles of igneous and metamorphic petrology: pearson new international edition*. 2. ed. Harlow: Pearson Education, 752 p.
- Yardley B. 1989. *An introduction to metamorphic petrology*. Harlow: Longman Earth Science Series, 248 p.